

Supporting Information

Electronic effect of a perfluorinated β -diketiminate ligand on the bonding nature of copper carbonyl complexes

*Kevin Huse, Hanns Weinert, Christoph Wölper, Stephan Schulz**

Content

I. NMR description of $^{17}\text{Fnac}_2\text{H}$ (**1**)

Scheme S1: Illustration isomers **1A - 1C**.

II. Calculated buried volume

Table S1: Calculated burried volumes for the model anions.

Scheme S2: Steric maps of L⁻ model anions.

III. Spectroscopic characterization

Fig. S1 - Fig. S9: ^1H , ^{13}C and ^{19}F NMR and mass spectra of $^{17}\text{Fnac}_2\text{H}$ (**1**).

Fig. S10 - Fig. S16: ^1H , ^{13}C and ^{19}F NMR of $^{17}\text{Fnac}_2\text{H}_-\text{NP}$ (**2**).

Fig. S17 - Fig. S21: ^1H , ^{13}C and ^{19}F NMR and IR spectra of $^{17}\text{Fnac}_2\text{CuC}_6\text{H}_6$ (**3**).

Fig. S22 - Fig. S28: ^1H , ^{13}C and ^{19}F NMR and IR spectra of $^{17}\text{Fnac}_2\text{CuCO}$ (**4**).

IV. Crystallographic details

Table S2: Crystallographic data of compounds **3** and **4**.

Fig S29: Molecular structure of $^{17}\text{Fnac}_2\text{CuC}_6\text{H}_6$ (**3a** and **3b**).

Table S3: Selected bond parameters for $^{17}\text{Fnac}_2\text{CuC}_6\text{H}_6$ (**3a** and **3b**).

V. Cyclic voltammetry

Fig S30: Overlay of cyclic voltammograms for LCuC₆H₆ complexes (L = $^{16}\text{Fnac}_2$, $^{17}\text{Fnac}_2$ (**3**); DCM/n-Bu₄BAr^F vs Fc^{0/+}).

Fig S31: Overlay of cyclic voltammograms for LCuC₆H₆ complexes (L = $^{16}\text{Fnac}_2$, $^{17}\text{Fnac}_2$ (**3**); DCM/n-Bu₄BAr^F vs Fc^{0/+}) over a wide scan range.

Tabel S4: Cyclic voltammetry data for LCuC₆H₆ complexes (L = $^{16}\text{Fnac}_2$, $^{17}\text{Fnac}_2$ (**3**), $^{18}\text{Fnac}_2$).

VI. Computational details

Fig S32: Illustration of NBOs for $^{17}\text{Fnac}_2\text{CuC}_6\text{H}_6$ (**3**).

Fig S33: Illustration of NBOs for $^{16}\text{Fnac}_2\text{CuCO}$.

Fig S34: Illustration of NBOs for $^{17}\text{Fnac}_2\text{CuCO}$ (**4**).

Table S5: Cartesian coordinates (x,y,z) for the optimized geometry of model anion Mesnac₂⁻.

Table S6: Cartesian coordinates (x,y,z) for the optimized geometry of model anion $^{16}\text{Fnac}_2^-$.

Table S7: Cartesian coordinates (x,y,z) for the optimized geometry of model anion $^{17}\text{Fnac}_2^-$.

Table S8: Cartesian coordinates (x,y,z) for the optimized geometry for $^{17}\text{Fnac}_2\text{C}_6\text{H}_6$.

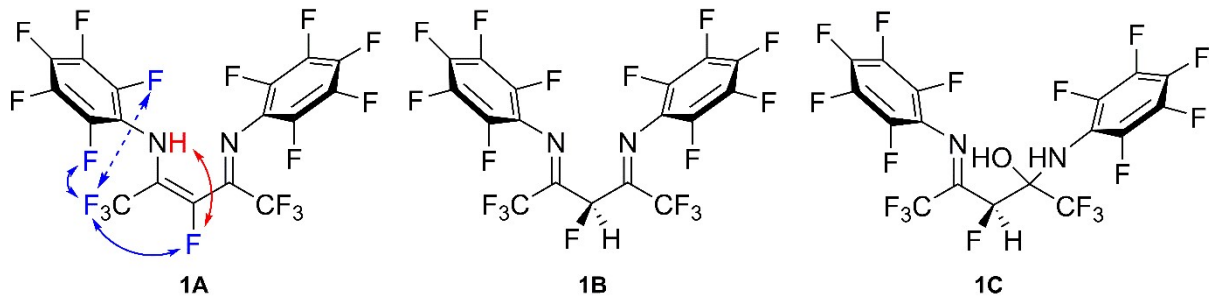
Table S9: Cartesian coordinates (x,y,z) for the optimized geometry for $^{17}\text{Fnac}_2\text{C}_6\text{H}_6$.

Table S10: Cartesian coordinates (x,y,z) for the optimized geometry for $^{17}\text{Fnac}_2\text{C}_6\text{H}_6$.

VII. References

I. NMR description $^{17}\text{F}\text{ac}_2\text{H}$ (1)

Signals were assigned via ^{19}F - ^{19}F -COSY NMR spectroscopy. The signals for the C_{2v} -symmetric isomer **1A** show the expected three resonances for the C_6F_5 substituents. While the signals for the *ortho*- and *para*-fluorine atoms of isomer **1A** are clearly separated at -150.94 ppm (d, $^3J_{\text{FF}} = 20.5$ Hz) and -163.28 ppm (m) respectively, the signals for the *meta*-fluorine atoms of isomer **1A** and **1B** overlap at 162.21 ppm (overl. m). The resonance of the γ -fluorine atom is found at -153.61 ppm (septd, $^4J_{\text{FF}} = 22.2$ Hz, $^2J_{\text{FH}} = 2.9$ Hz) as a septet of doublets. The septet splitting results from $^4J_{\text{FF}}$ -coupling to the magnetically equivalent CF_3 -groups in the ligand backbone, the doublet-splitting is due to $^4J_{\text{FH}}$ through-space coupling to the NH proton in the enamine-imine structure ($^4J_{\text{FH}} = 2.9$ Hz). The magnetically equivalent CF_3 groups for isomer **1A** appear as doublets of triplets at -65.08 ppm (dt, $^4J_{\text{FF}} = 22.2$ Hz, $^6J_{\text{FF}} = 3.6$ Hz, 6F), the doublet splitting resulting from $^4J_{\text{FF}}$ coupling of the CF_3 -groups with the γ -fluorine atom. The triplet splitting is due to through space interaction of the CF_3 group with the two *ortho*-fluorine atoms in close proximity, which could be detected by ^{19}F - ^{19}F COSY NMR spectroscopy (see Figure S5) and was also detected for a similar ligand.^[1]



Scheme S1: Illustration of the $^4J_{\text{FF}}$ and through-space coupling partners in isomer **1A**. Highlighted in blue are the coupling partners responsible for the doublet of triplet splitting for the CF_3 -groups, highlighted in red is the through space coupling interaction responsible for the doublet splitting of the NH proton (^1H NMR) and the doublet splitting of the septet for the γ -fluorine atom (^{19}F NMR).

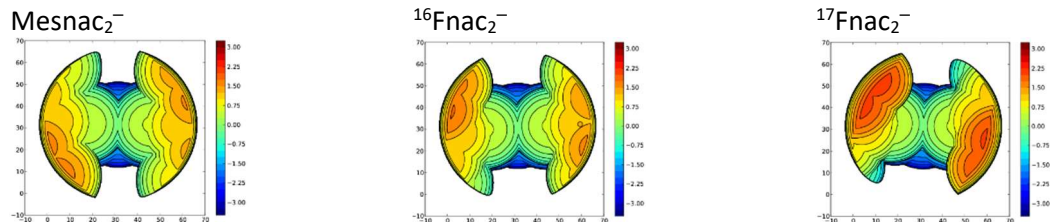
The ^{19}F NMR spectrum of isomer **1B** shows no higher symmetry. Two distinct singlet signals for the CF_3 -groups indicate the missing of a mirror plain in the molecule structure in solution. The γ -fluorine atom appears at higher field at -128.46 ppm as a singlet, which indicates bonding to a sp^3 -hybridized carbon atom as drawn in Scheme S1. This is further supported by the shift of the remaining proton in the ^1H NMR spectrum, which appears at 3.96 ppm, eliminating the possibility for a N-H group and hinting towards a C-H group. The C_6F_5 groups show two sets of signals [-150.42 (d, $^3J_{\text{FF}} = 19.3$ Hz, 2F, o-F), -151.57 (d, $^3J_{\text{FF}} = 19.5$ Hz, 2F, o-F), -156.50 (overl. t, $^3J_{\text{FF}} = 21.4$ Hz, 1F, p-F), -156.60 (overl. t, $^3J_{\text{FF}} = 21.7$ Hz, 2F, m-F), -158.48 (t, $^3J_{\text{FF}} = 21.7$ Hz, 1F, p-F), -162.21 (overl. m, 2F, m-F)]. While these are the main isomers in solution, additional isomers are present in the ^{19}F NMR spectrum. Variable temperature NMR spectroscopy studies carried out between -80 °C to 60 °C in chloroform- d_1 did not show any signs of a temperature dependent equilibrium. However, addition of sulfuric acid to a

solution of $^{17}\text{Fnac}_2\text{H}$ in benzene- d_6 resulted in an incomplete shift of the isomer ratio towards isomer **1B**. Low resolution mass spectrometry of LH only shows the M and M^- fragments expected for the ligand, whereas no peak corresponding to the hemiaminal **1C** is detected. Upon solvation in DMSO- d_6 all isomers quantitatively undergo the cyclisation reaction with hydrogen fluoride elimination (see Figure S10). The reason for the magnetically inequivalent CF_3 groups as well as for the aryl substituents for isomer **1B** thus remains unknown.

II. Calculated buried volume

Table S1: Calculated buried volumes for the model anions Mesnac_2^- , $^{16}\text{Fnac}_2^-$, and $^{17}\text{Fnac}_2^-$.

Complex	V_{buried}	V_{free}
Mesnac_2^-	53.7	46.0
$^{16}\text{Fnac}_2^-$	49.6	50.4
$^{17}\text{Fnac}_2^-$	51.6	48.4



Scheme S2: Steric maps of L^- model anions Mesnac_2^- , $^{16}\text{Fnac}_2^-$ and $^{17}\text{Fnac}_2^-$ derived from solid state structures of appropriate $\text{Fnac}_2\text{Cu-R}$ complexes. The corresponding copper atom was chosen as the spheres center and the sphere radius was set to 3.5 Å.

III. Spectroscopic characterization

a) Spectra of $^{17}\text{Fnac}_2\text{H}$ (1)

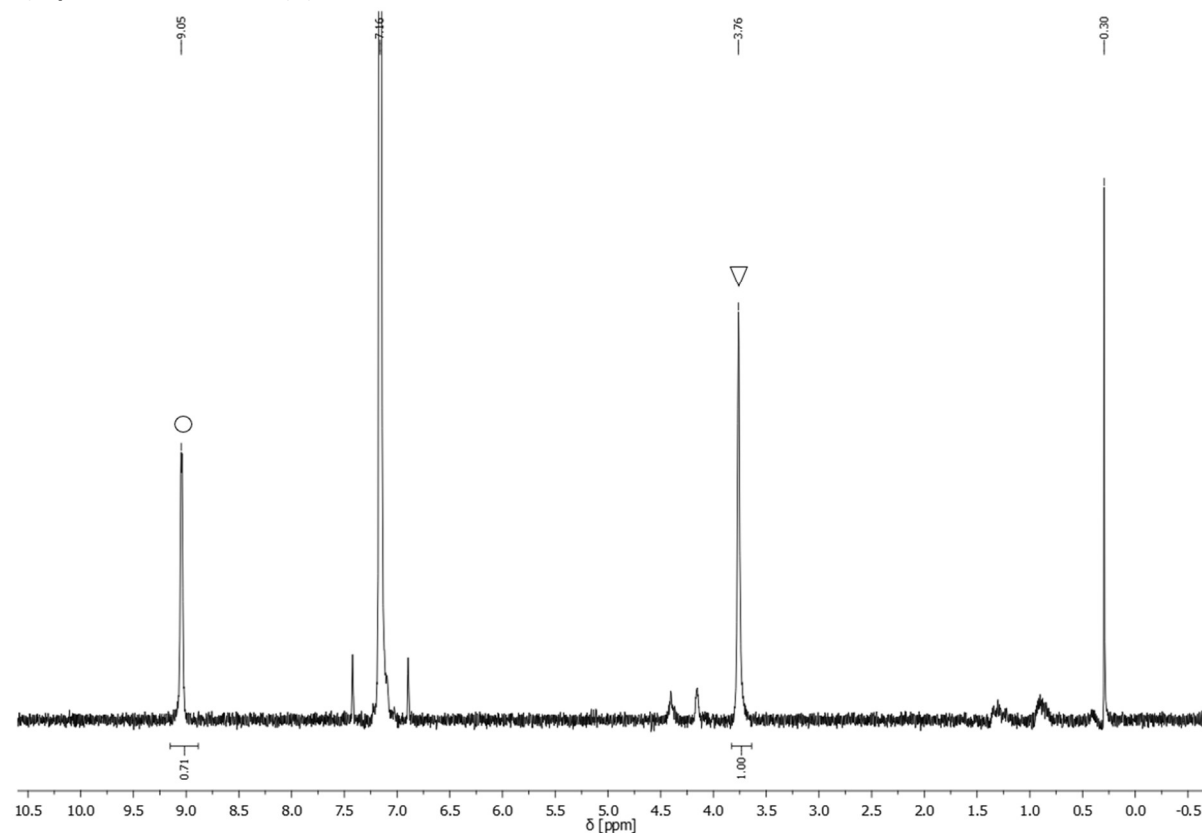


Fig. S1: ^1H NMR of $^{17}\text{Fnac}_2\text{H}$ (Isomer A(○), Isomer B(▽)) in benzene- d_6 at room temperature.

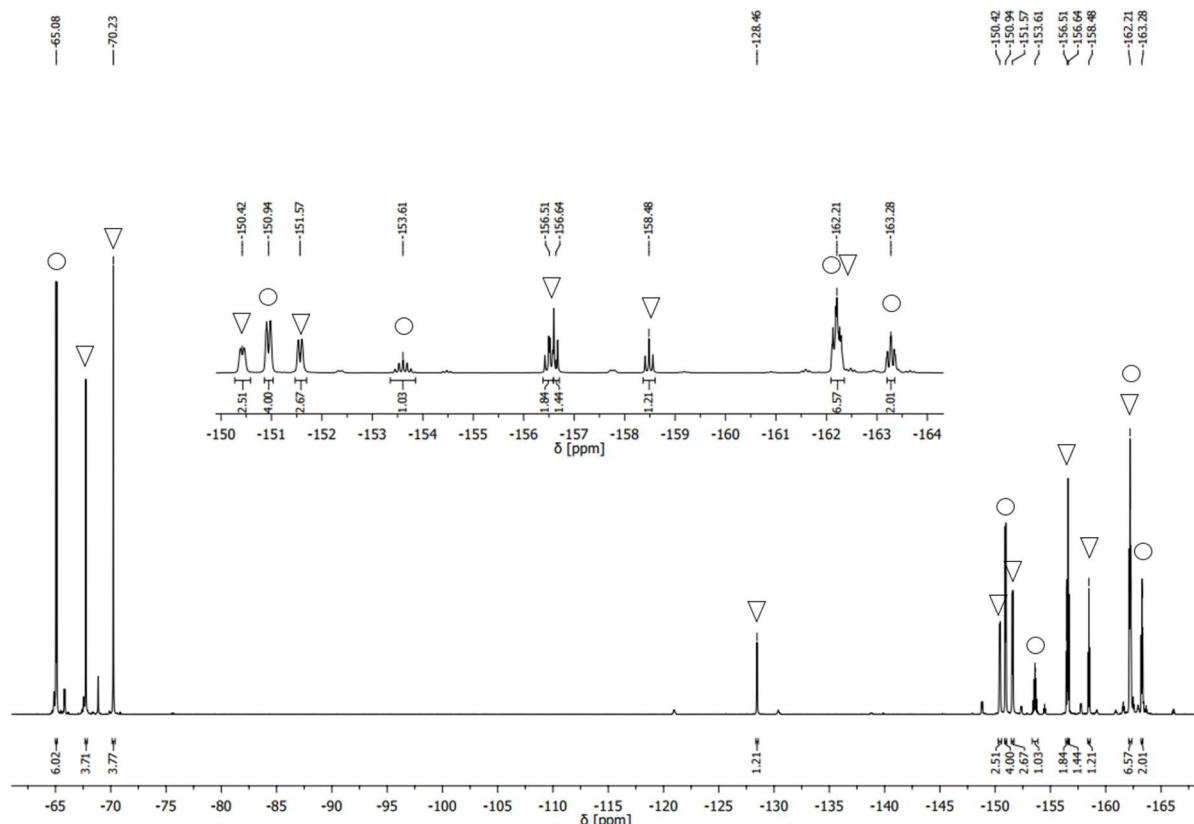


Fig. S2: ^{19}F NMR of $^{17}\text{Fnac}_2\text{H}$ (Isomer A(○) Isomer B(▽)) in benzene- d_6 at room temperature.

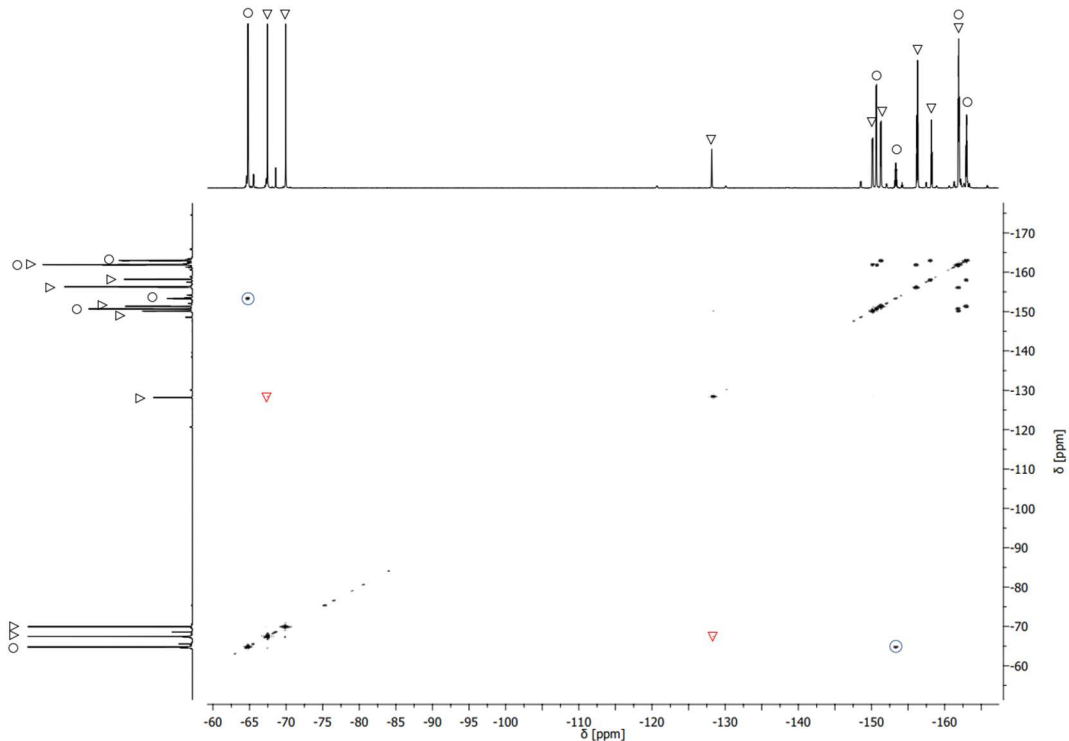


Fig. S3: ^{19}F - ^{19}F -COSY NMR spectrum of ligand $^{17}\text{Fnac}_2\text{H}$ in benzene- d_6 at room temperature. The signals resulting from CF_3 - γ -F interactions are highlighted. Symbols indicate the isomers **A** and **B** as mentioned before.

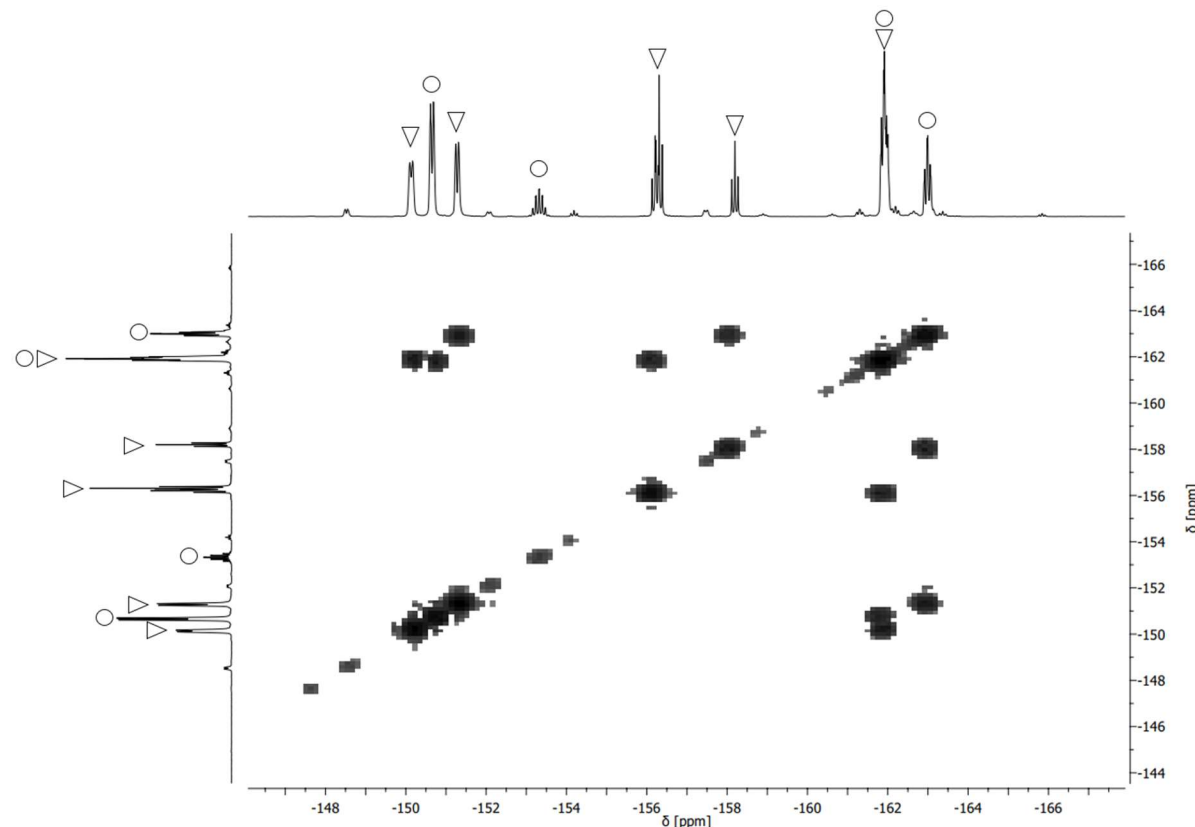


Fig. S4: Aromatic region of the ^{19}F - ^{19}F COSY NMR spectrum of ligand $^{17}\text{Fnac}_2\text{H}$ in benzene- d_6 at room temperature. Symbols indicate the isomers **A** and **B** as mentioned before.

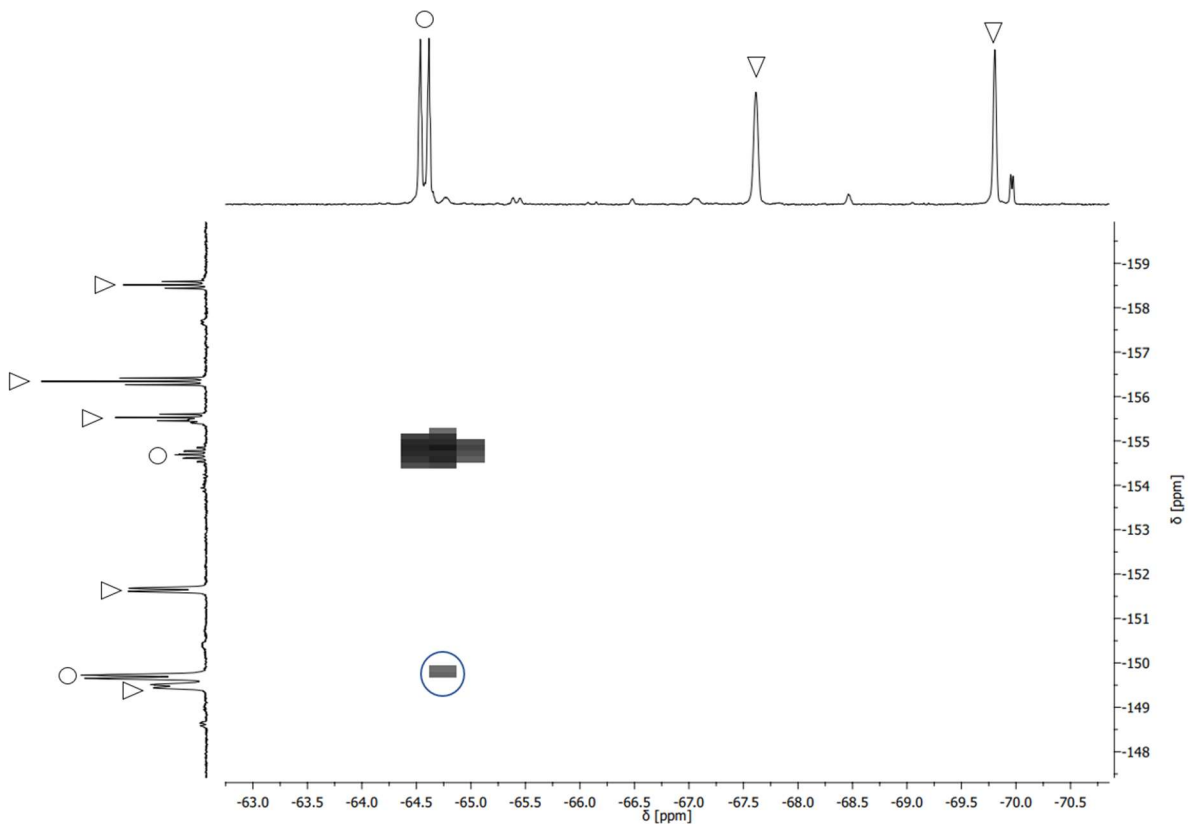


Fig. S5: Correlation between the CF₃-groups and the *ortho*-fluorine atoms of isomer **1A** in the ¹⁹F-¹⁹F COSY NMR spectrum measured in CDCl₃ at room temperature.

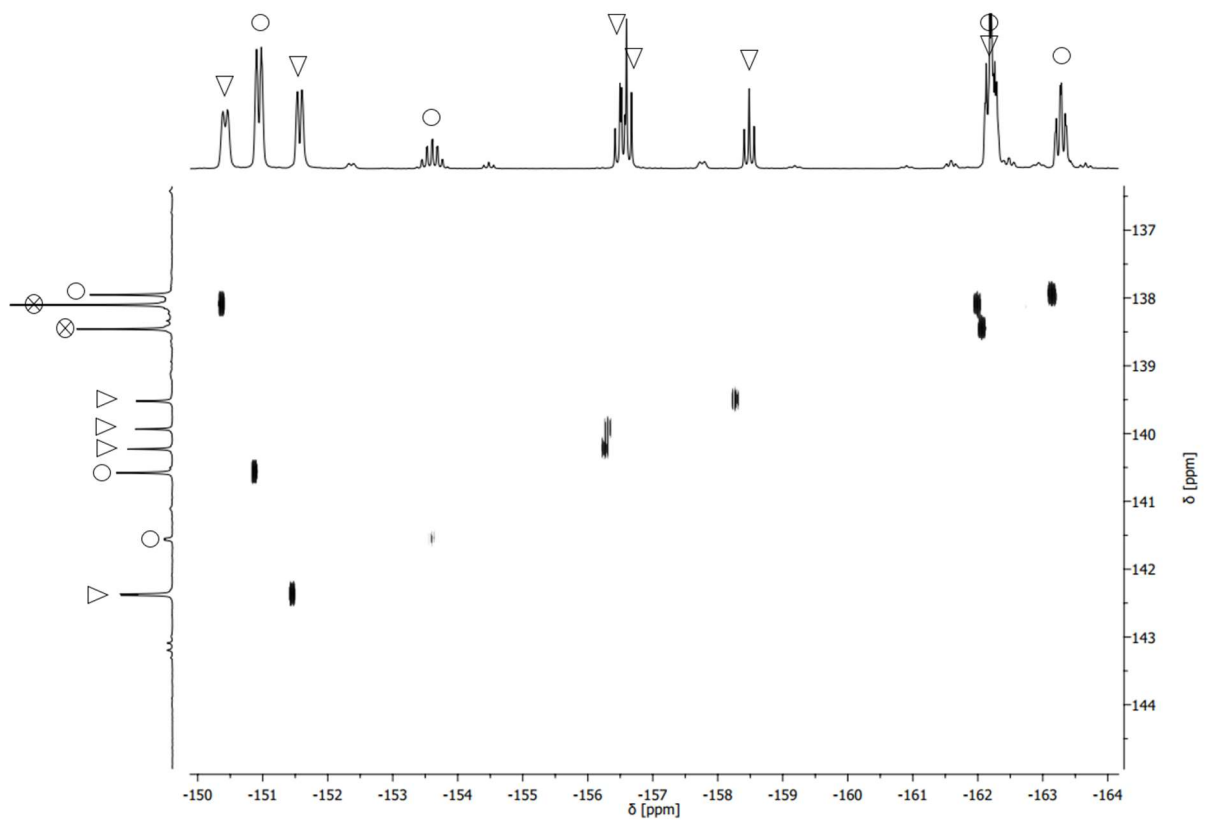


Fig. S6: ¹³C-¹⁹F HMQC NMR of ¹⁷Fnac₂H (Isomer A(○), Isomer B(▽)) for the aromatic region in benzene-d₆ at room temperature.

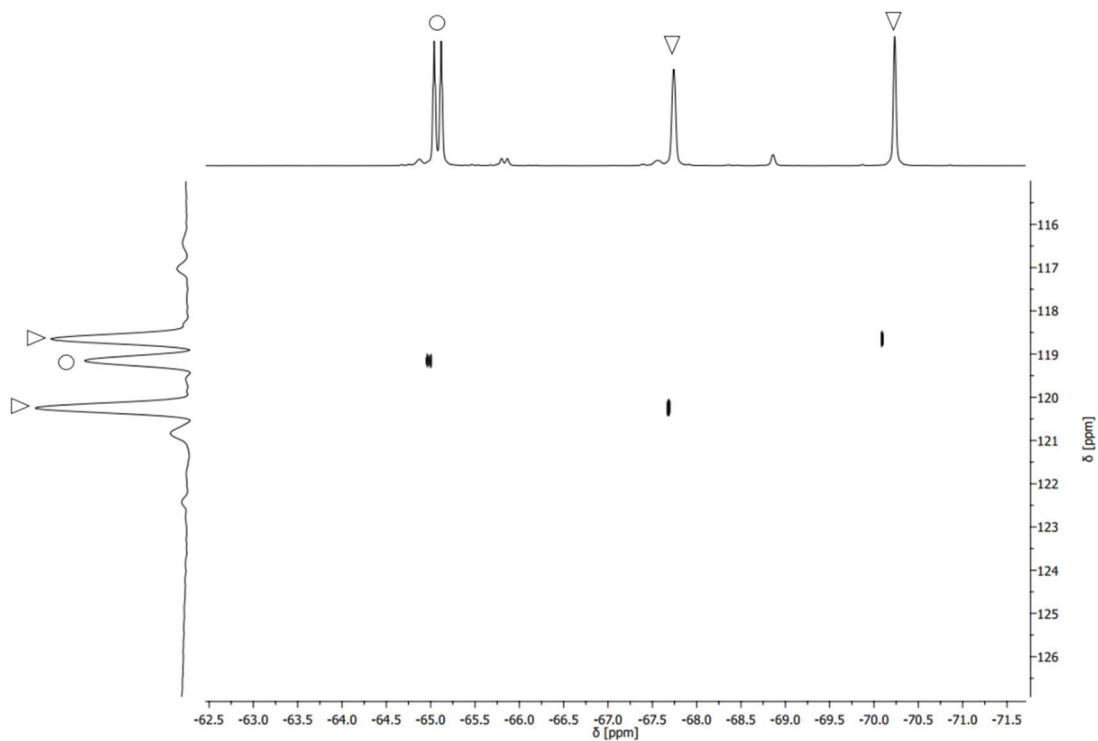


Fig. S7: ^{13}C - ^{19}F HMQC NMR of $^{17}\text{Fnac}_2\text{H}$ (Isomer A(\circ), Isomer B(∇)) for the aliphatic region in benzene- d_6 at room temperature.

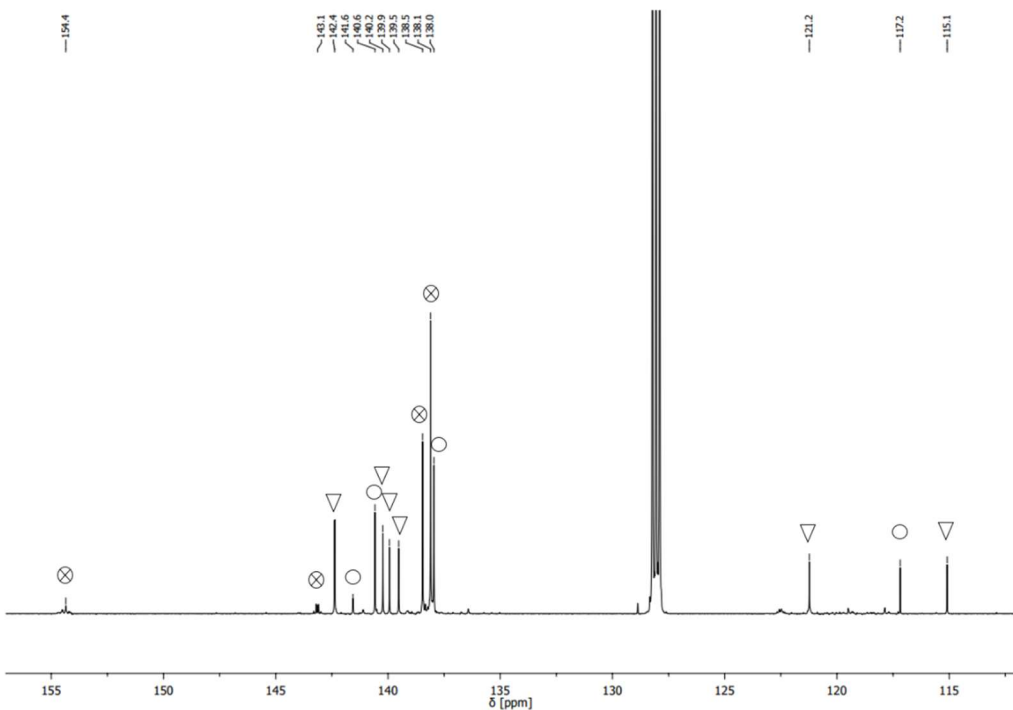


Fig. S8: $^{13}\text{C}\{^{19}\text{F}\}$ NMR of $^{17}\text{Fnac}_2\text{H}$ (isomer A(\circ)), isomer B(∇), non-assignable (\otimes)) in benzene- d_6 at room temperature.

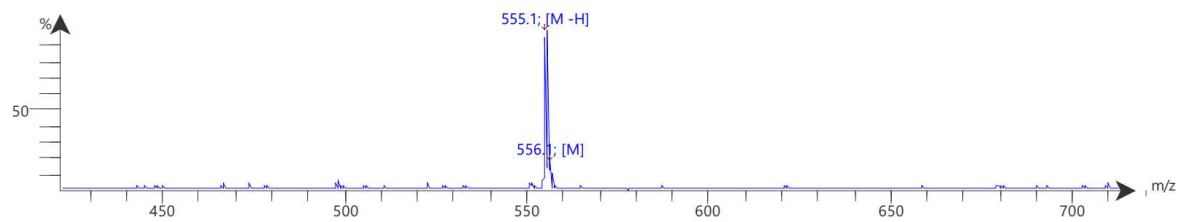


Fig. S9: Mass spectrum of $^{17}\text{Fnac}_2\text{H}$.

b) Spectra of cyclic byproduct $^{17}\text{Fnac}_2\text{H}_\text{NP}$ (2)

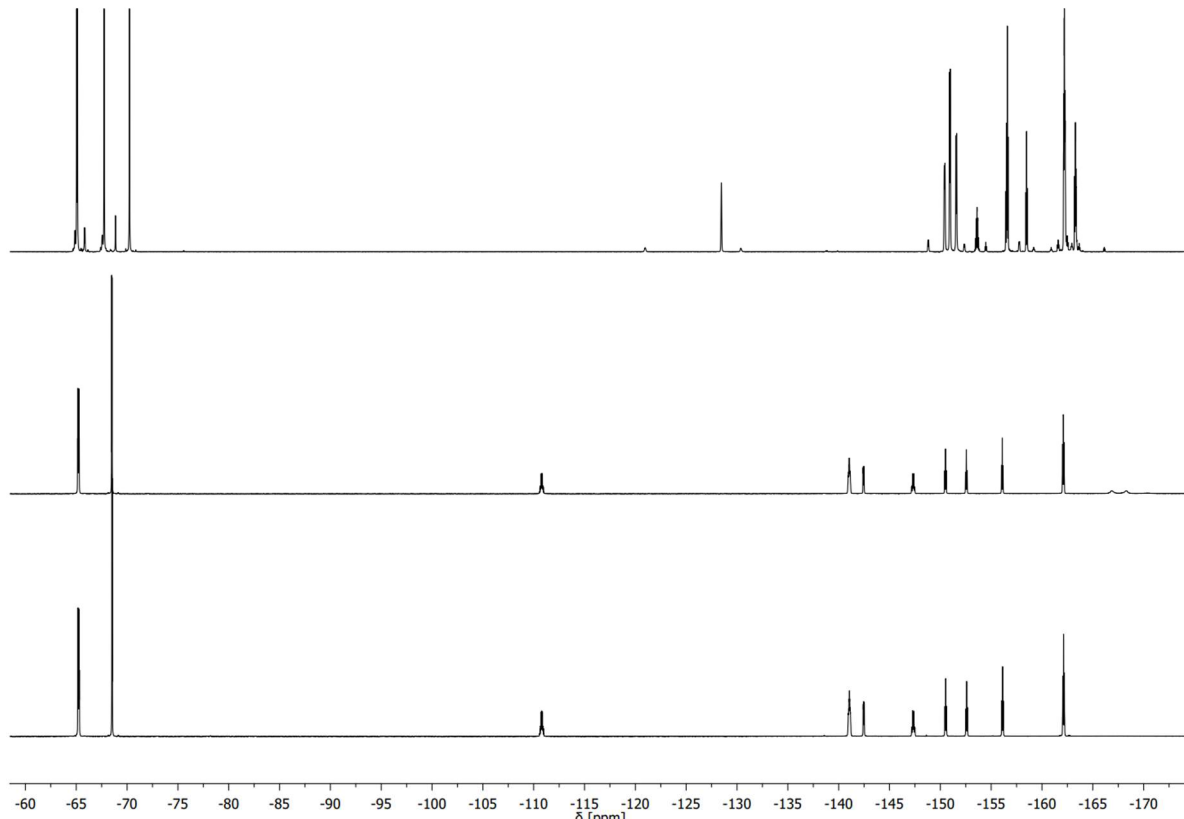


Fig. S10: Formation of **2** under HF elimination. Top: **1** in C_6D_6 . Middle: Addition of $\text{DMSO}-d_6$ to **1** yields **2** with HF elimination (doublet at 167.57 ppm). Bottom: Same sample after application of vacuum.

The chemical shift of HF as well as the signal structure strongly depends on the measuring conditions, as concentration and temperature greatly affect the degree of oligomerization of HF and therefore have a large influence on the chemical shift of the detected ^{19}F NMR signals. For a detailed study on the effect of temperature and concentration on the appearance of the NMR signals of HF, see the following references: a) J. Shamir, A. Netzer, *N.M.R. Studies of Anhydrous Hydrogen Fluoride Solutions*, CAN. J. CHEM. VOL. 51, 1973, 2676. b) I. G. Shenderovich, S. N. Smirnov, G. S. Denisov, V.A. Gindin, N. S. Golubev, A. DUnger, R. Reibke, S. Kirpekar, O. L. Malkina, H. H. Limbach, *Nuclear Magnetic Resonance of Hydrogen Bonded Clusters Between F^- and $(\text{HF})_n$: Experiment and Theory*, Ber. Bunsenges. Phys. Chem. 102, 422–428 (1998) No. 3.

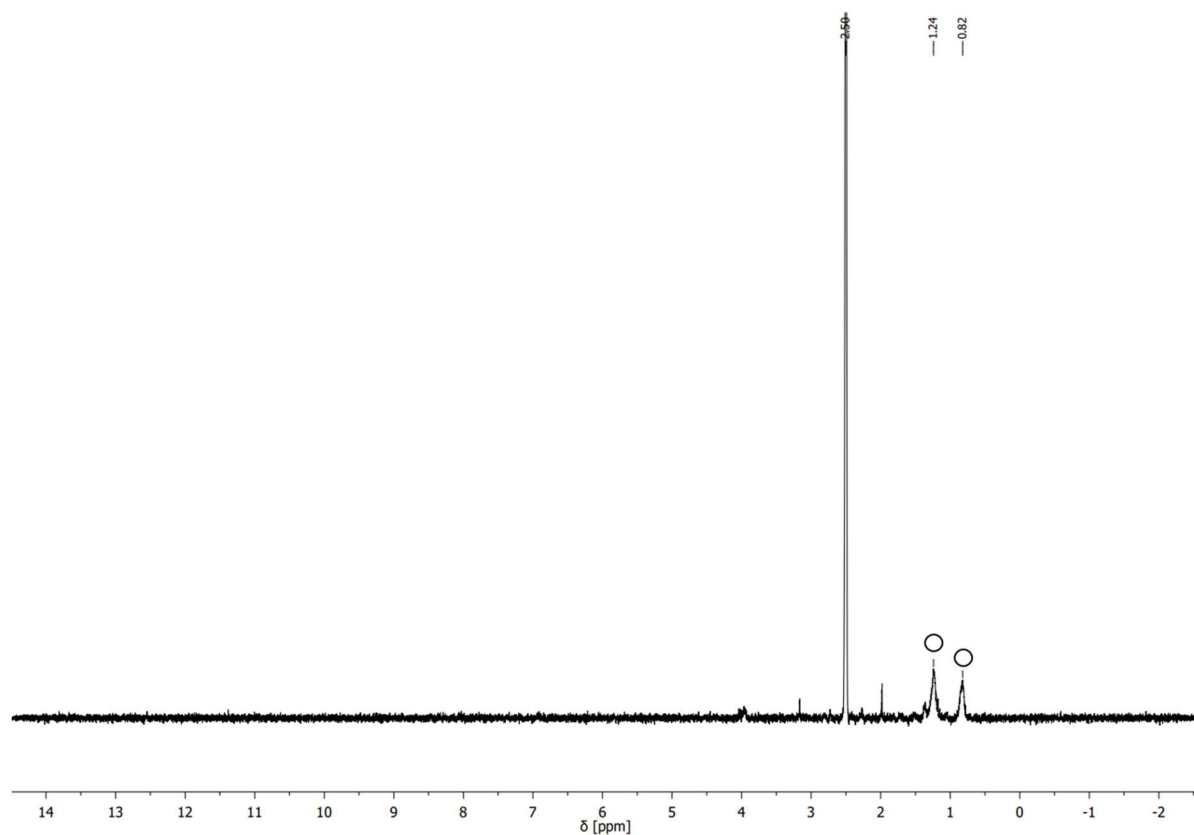


Fig. S11: ^1H NMR spectrum of $^{17}\text{Fnac}_2\text{H_NP}$ in $\text{DMSO}-d_6$ at room temperature. Signals marked with \bigcirc belong to *n*-hexane.

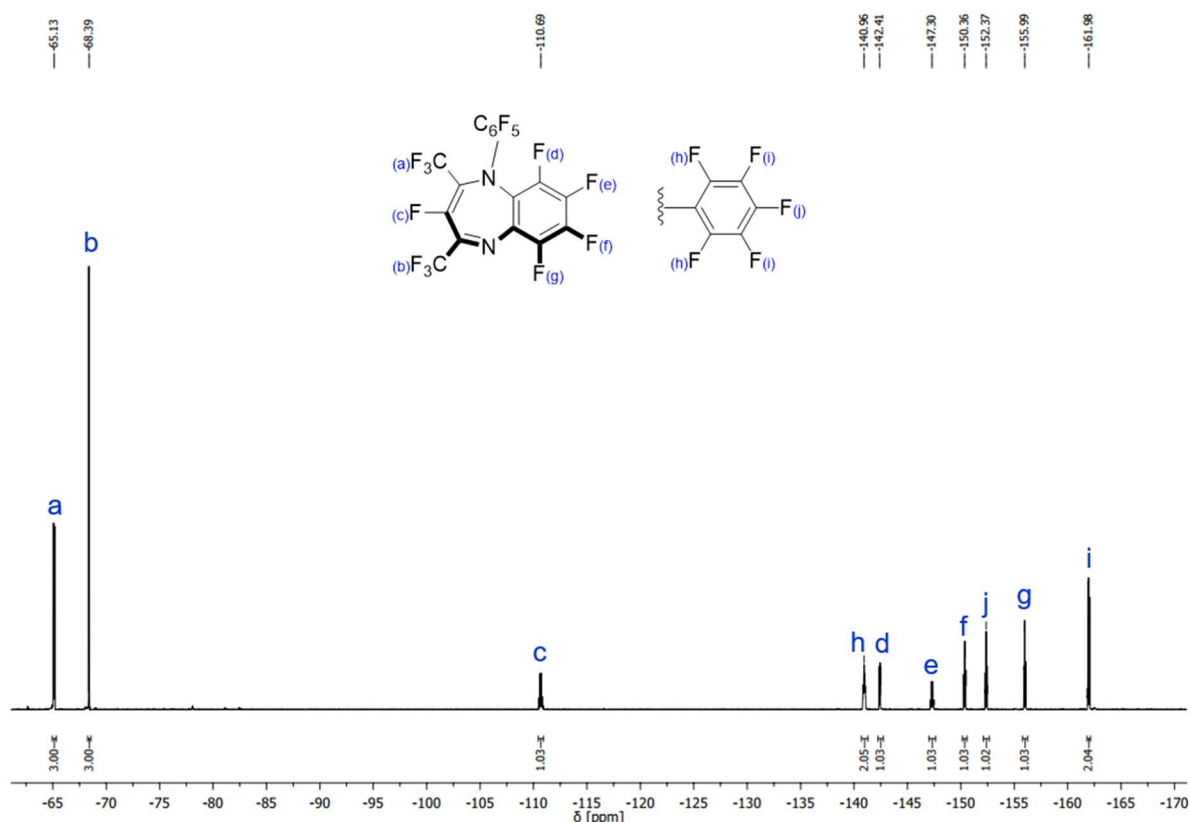


Fig. S12: ^{19}F NMR spectrum of $^{17}\text{Fnac}_2\text{H_NP}$ in $\text{DMSO}-d_6$ at room temperature.

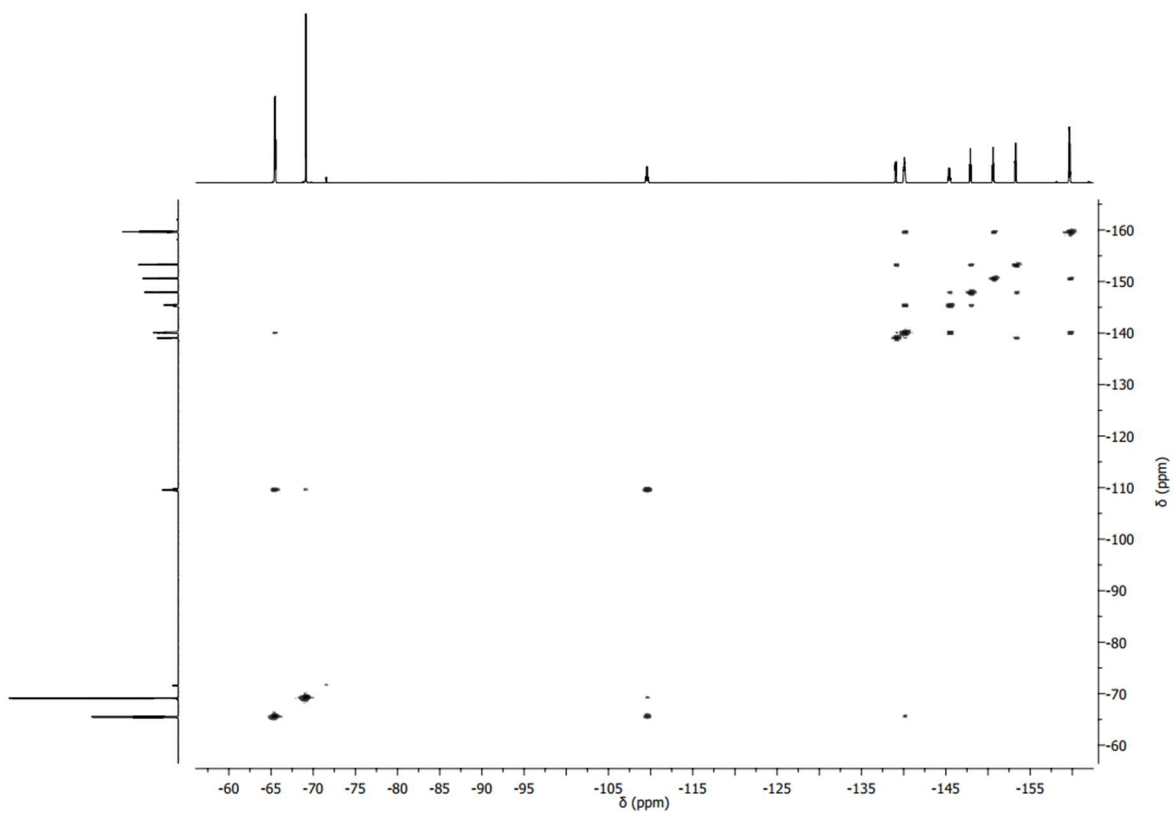


Fig. S13: ^{19}F - ^{19}F COSY NMR spectrum of $^{17}\text{Fnac}_2\text{H_NP}$ in $\text{DMSO}-d_6$ at room temperature.

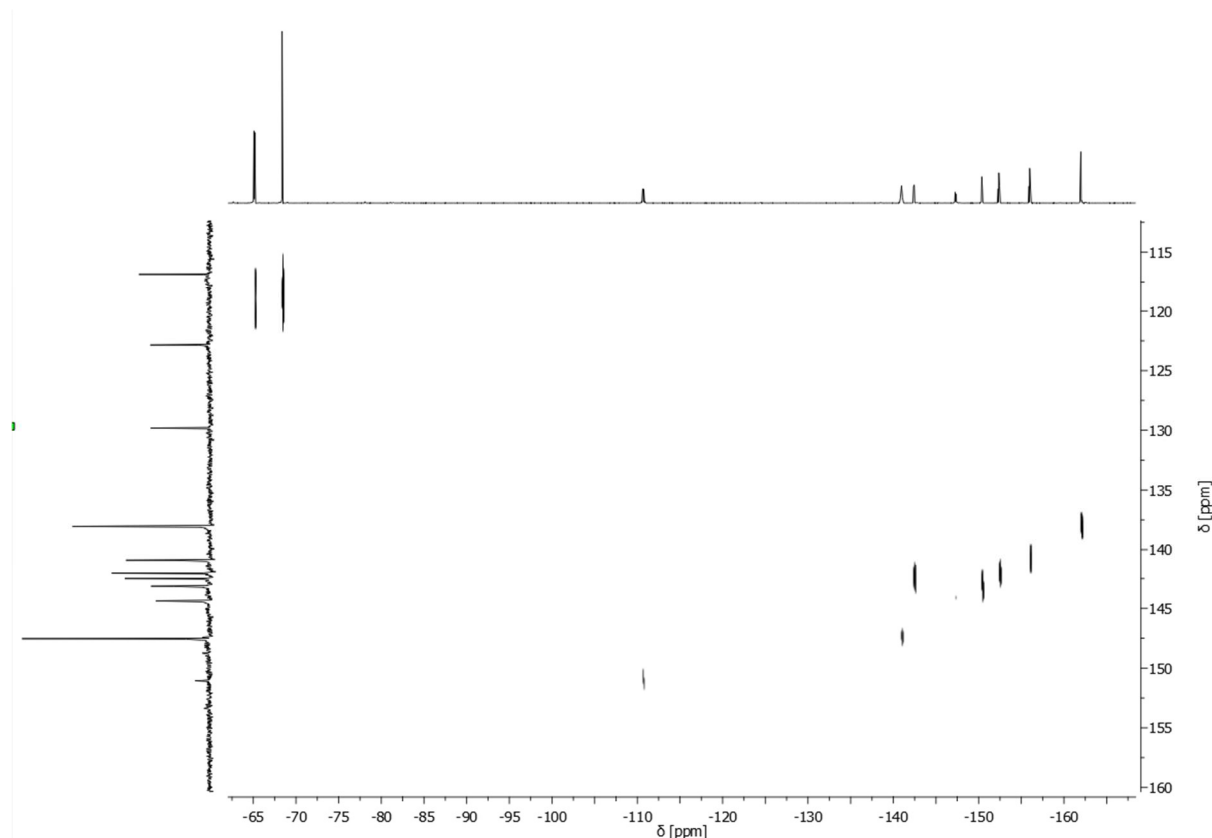


Fig. S14: ^{13}C - ^{19}F HMQC NMR spectrum of $^{17}\text{Fnac}_2\text{H_NP}$ in $\text{DMSO}-d_6$ at room temperature.

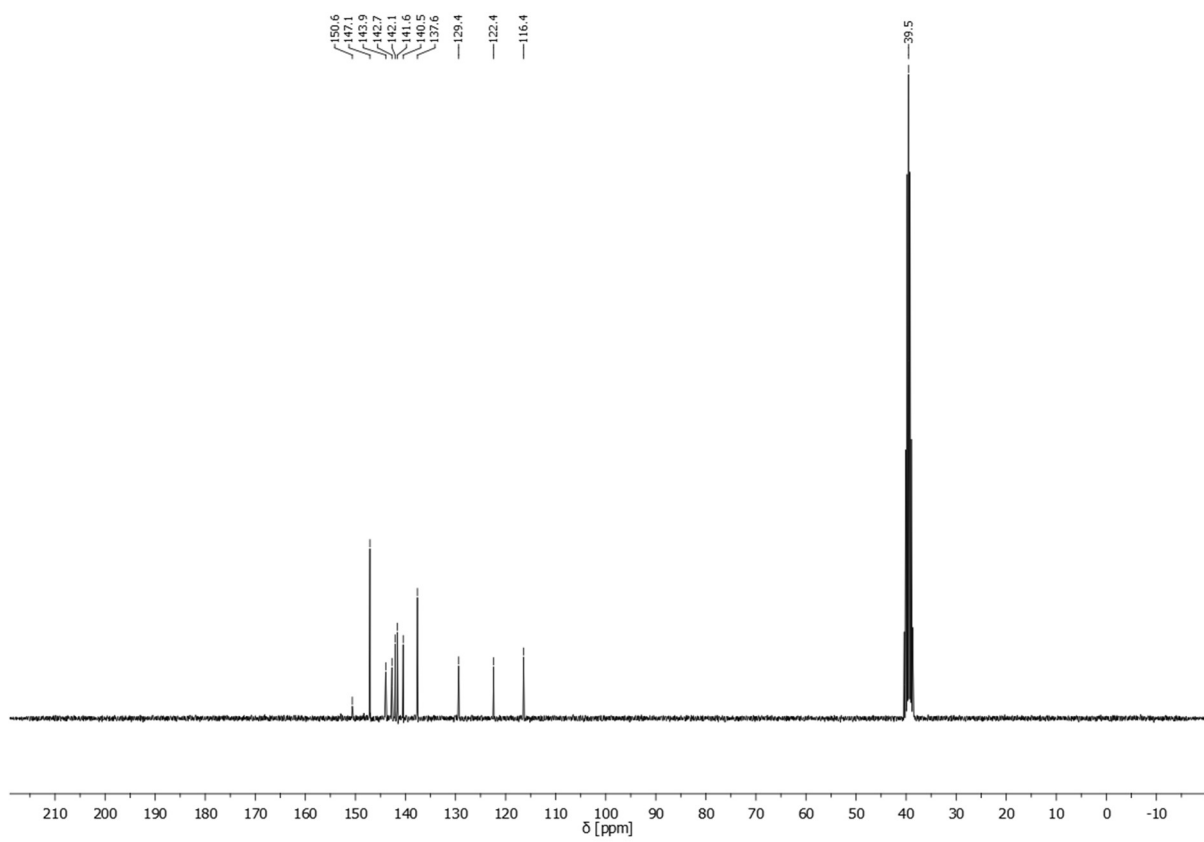


Fig. S15: $^{13}\text{C}\{^{19}\text{F}\}$ NMR spectrum of $^{17}\text{Fnac}_2\text{H_NP}$ in $\text{DMSO}-d_6$ at room temperature.

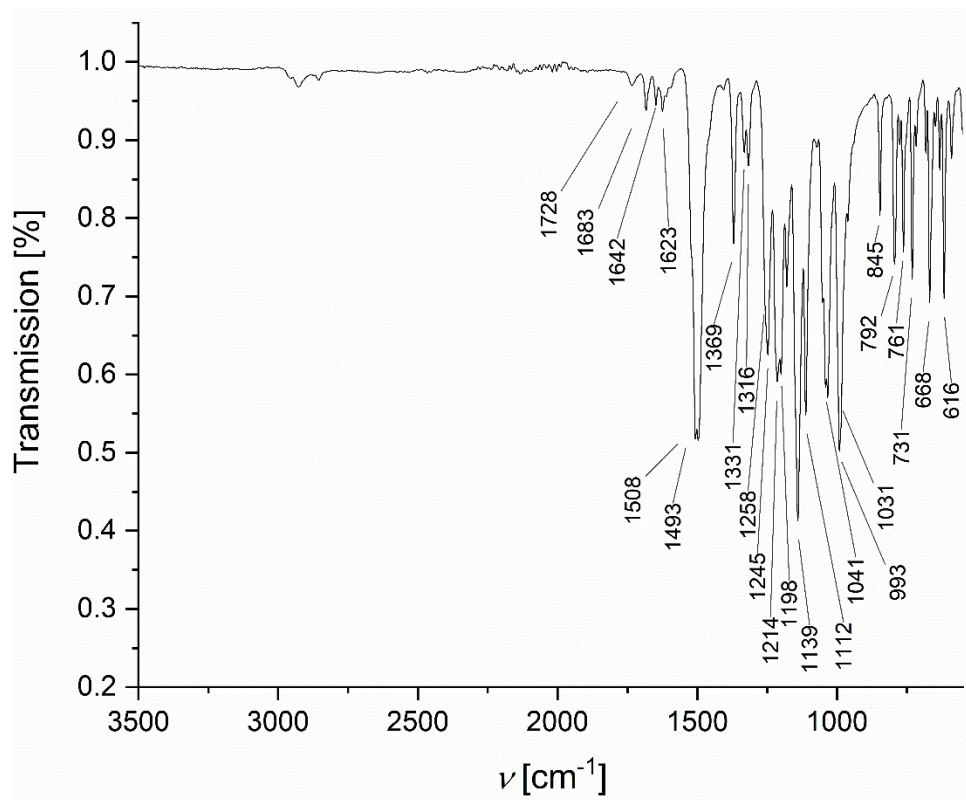


Fig. S16: ATR-IR spectrum of $^{17}\text{Fnac}_2\text{NP}$.

c) Spectra of $^{17}\text{Fnac}_2\text{CuC}_6\text{H}_6$ (3)

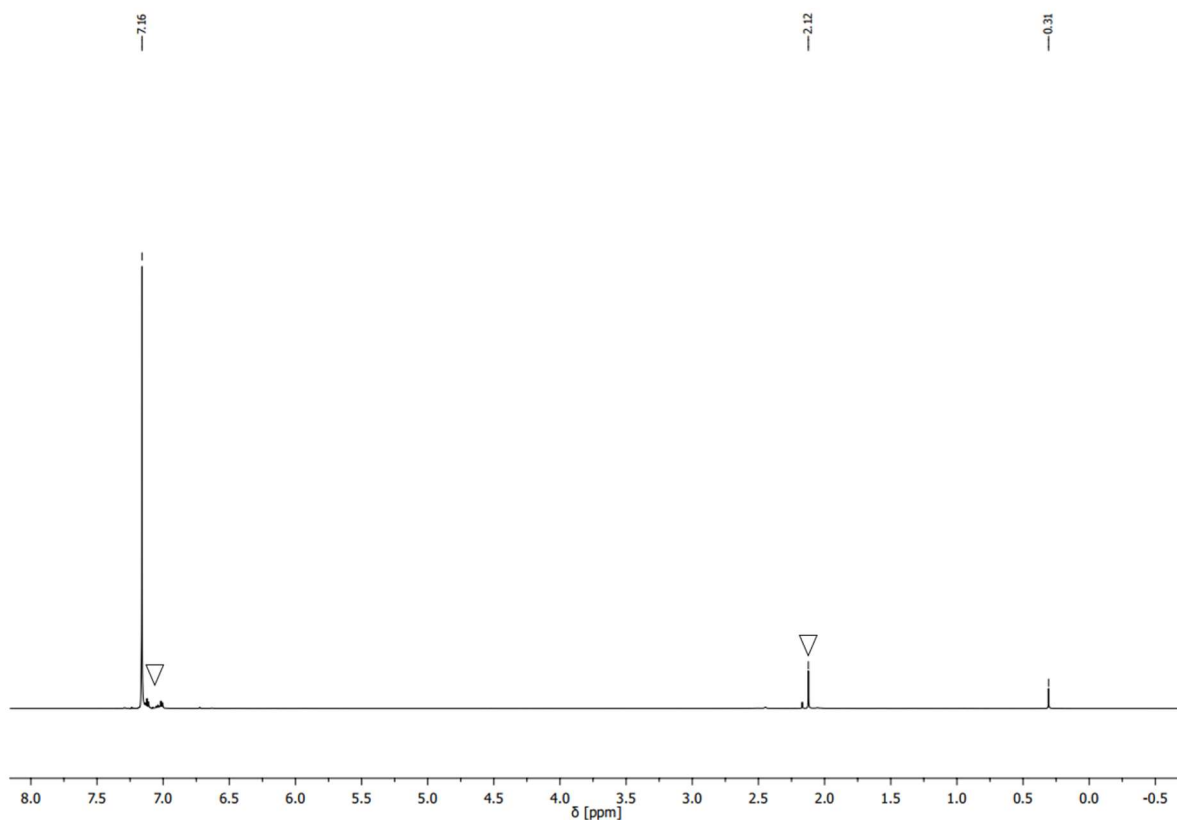


Fig. S17: ^1H NMR $^{17}\text{Fnac}_2\text{CuC}_6\text{D}_6$ in benzene- d_6 at room temperature. Signals marked with ∇ belong to mesitylene.

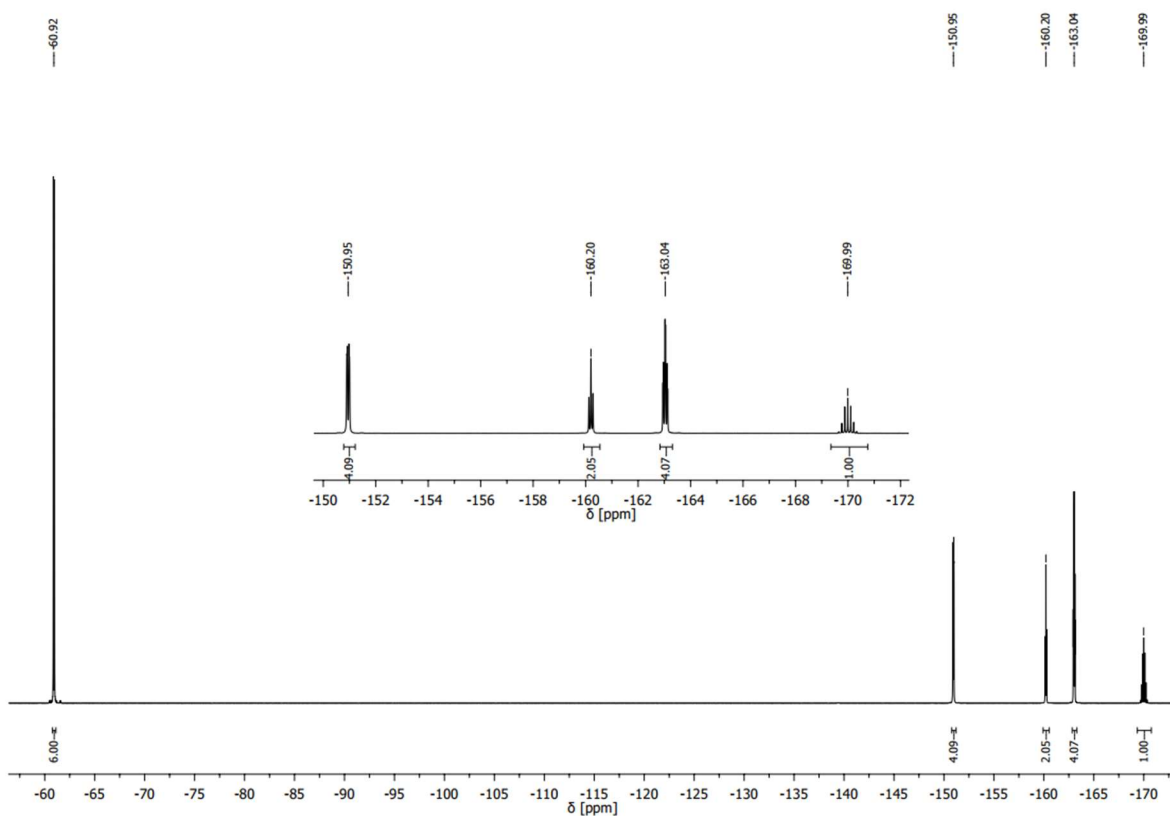


Fig. S18: ^{19}F NMR of $^{17}\text{Fnac}_2\text{CuC}_6\text{D}_6$ in benzene- d_6 at room temperature.

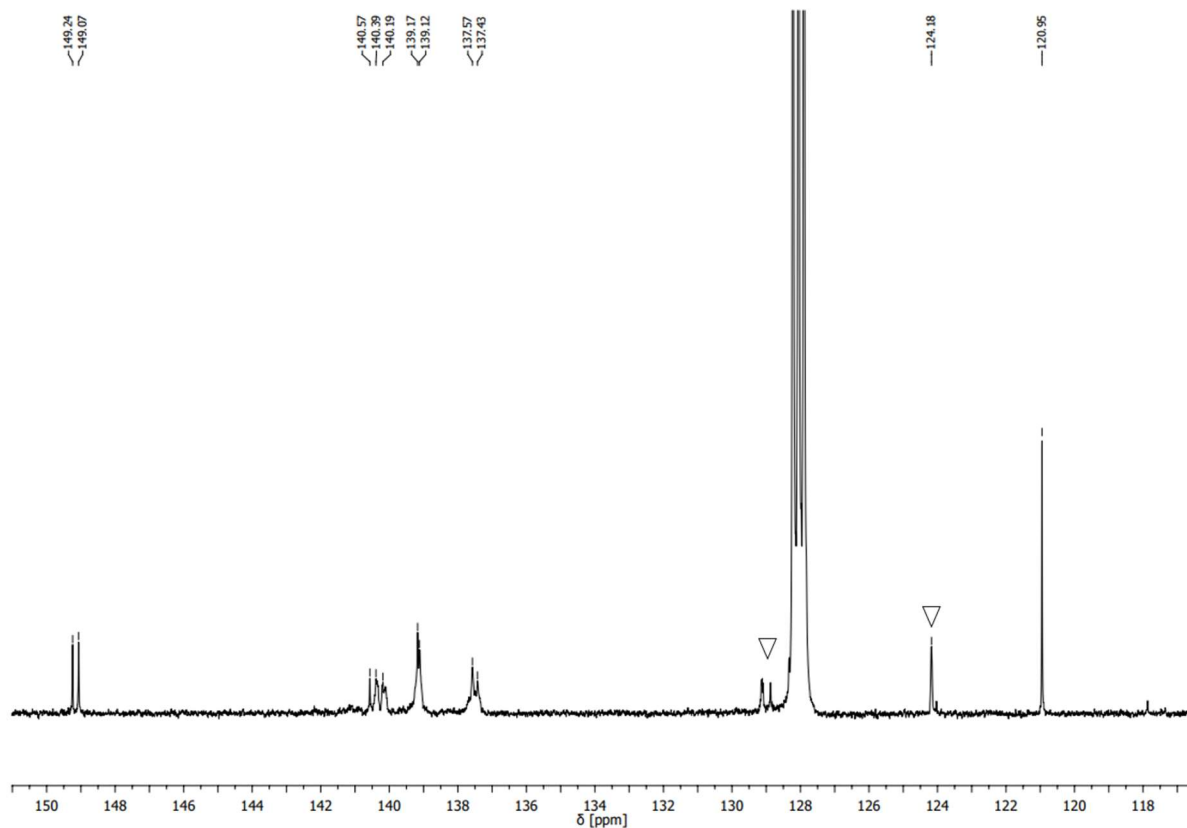


Fig. S19: $^{13}\text{C}\{^{19}\text{F}\}$ NMR of $^{17}\text{Fnac}_2\text{CuC}_6\text{D}_6$ in benzene- d_6 at room temperature with ^{19}F decoupling pulse at -60 ppm. Signals marked with ∇ belong to mesitylene.

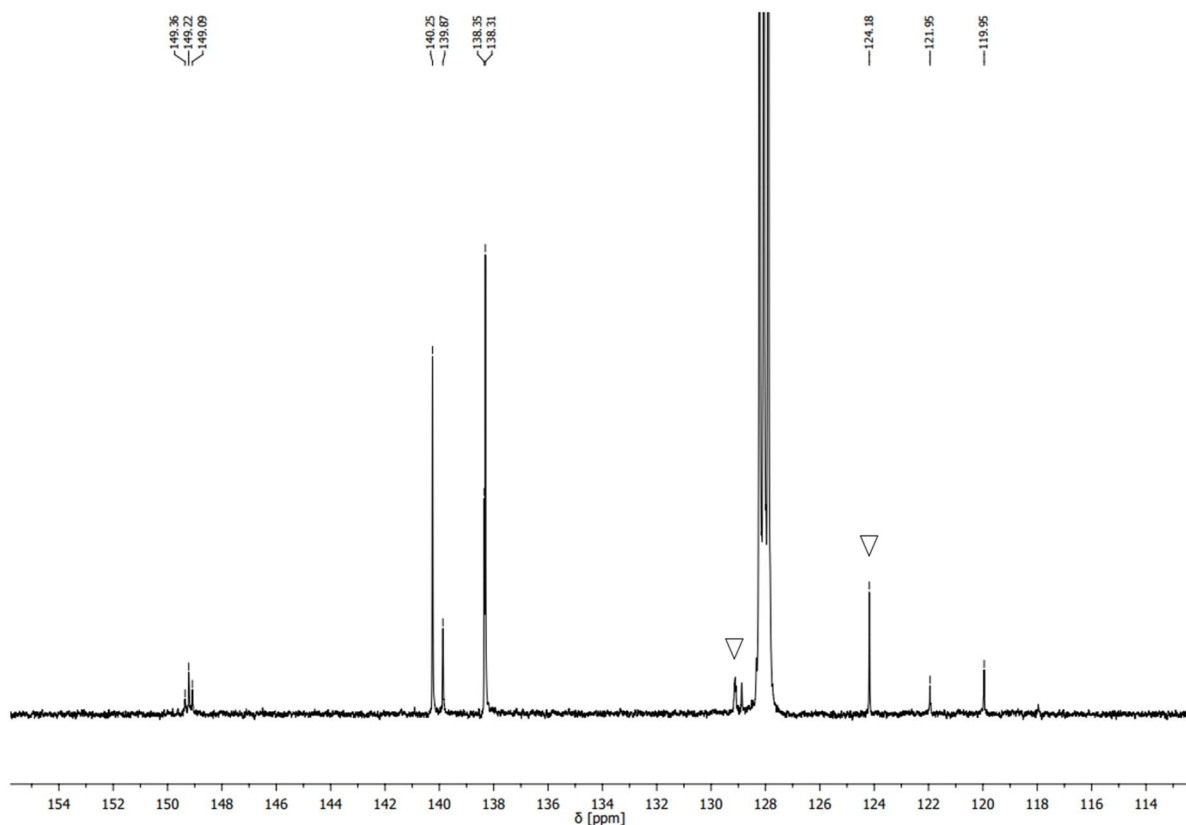


Fig. S20: $^{13}\text{C}\{^{19}\text{F}\}$ NMR of $^{17}\text{Fnac}_2\text{CuC}_6\text{D}_6$ in benzene- d_6 at room temperature with ^{19}F decoupling pulse at -110 ppm. Signals marked with ∇ belong to mesitylene.

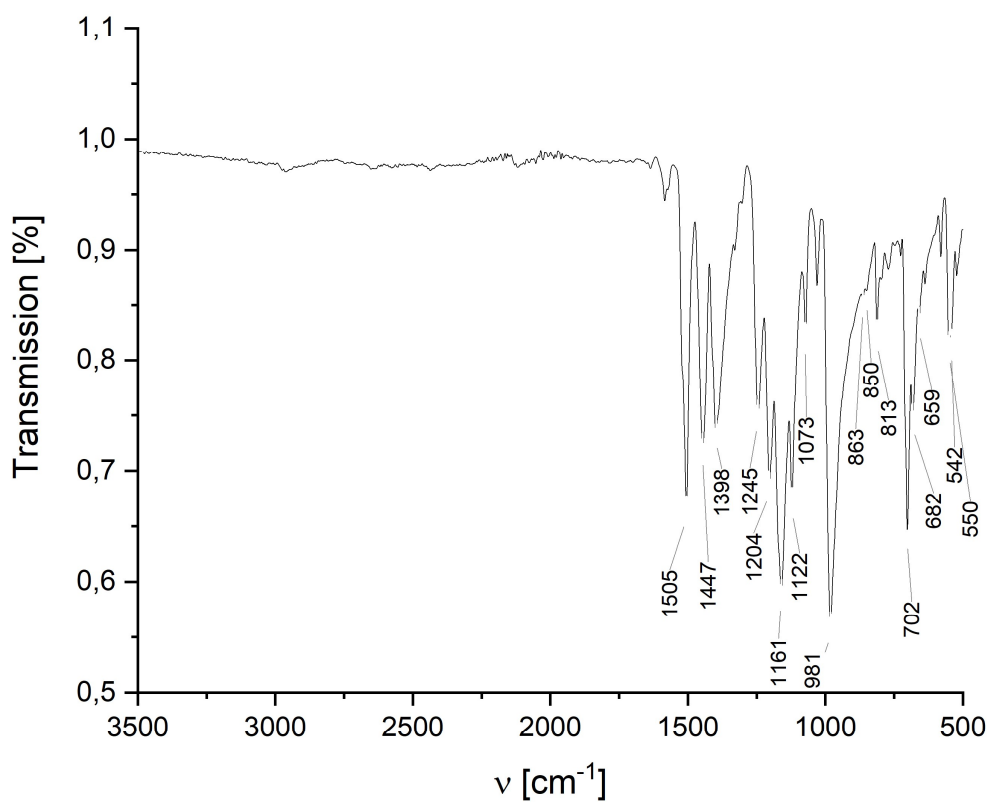


Fig. S21: ATR-IR spectrum of $^{17}\text{Fnac}_2\text{CuC}_6\text{H}_6$.

d) Spectra of $^{17}\text{Fnac}_2\text{CuCO}$ (4)

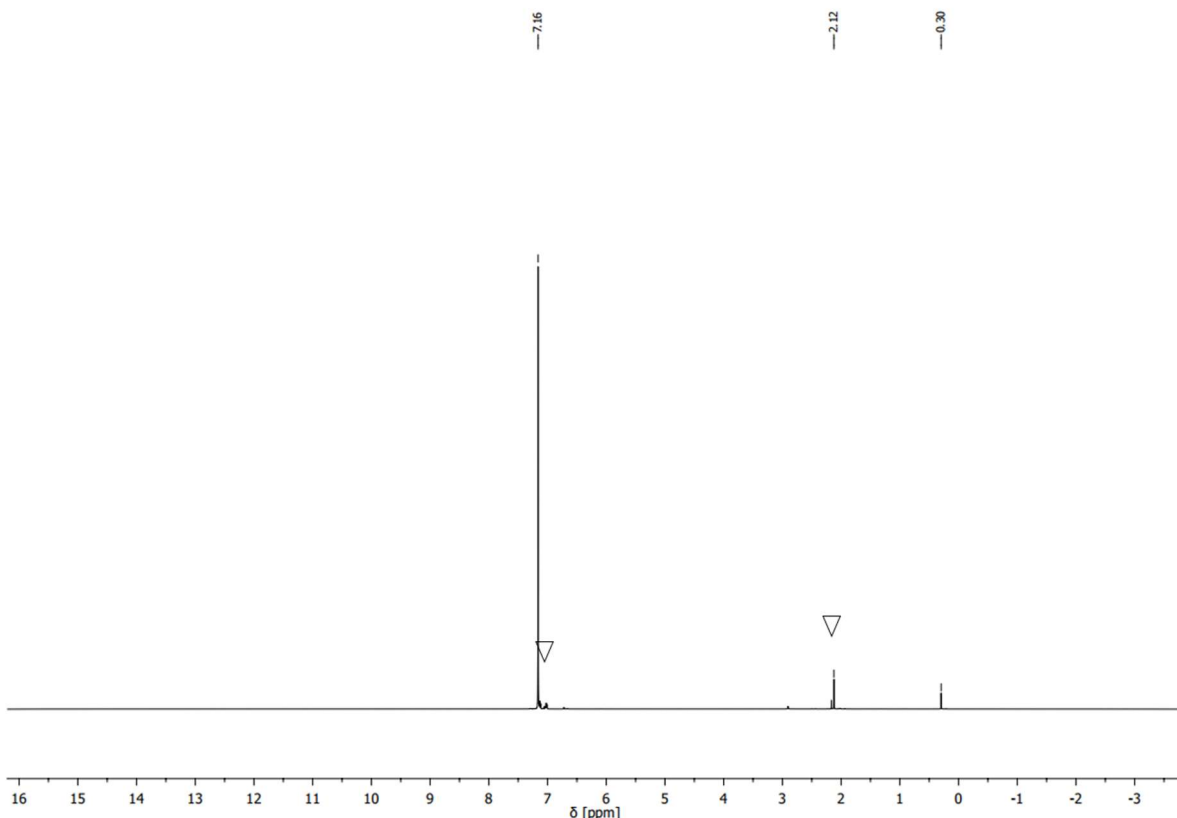


Fig. S22: ^1H NMR $^{17}\text{Fnac}_2\text{CuCO}$ in benzene- d_6 at room temperature. Signals marked with ∇ belong to mesitylene.

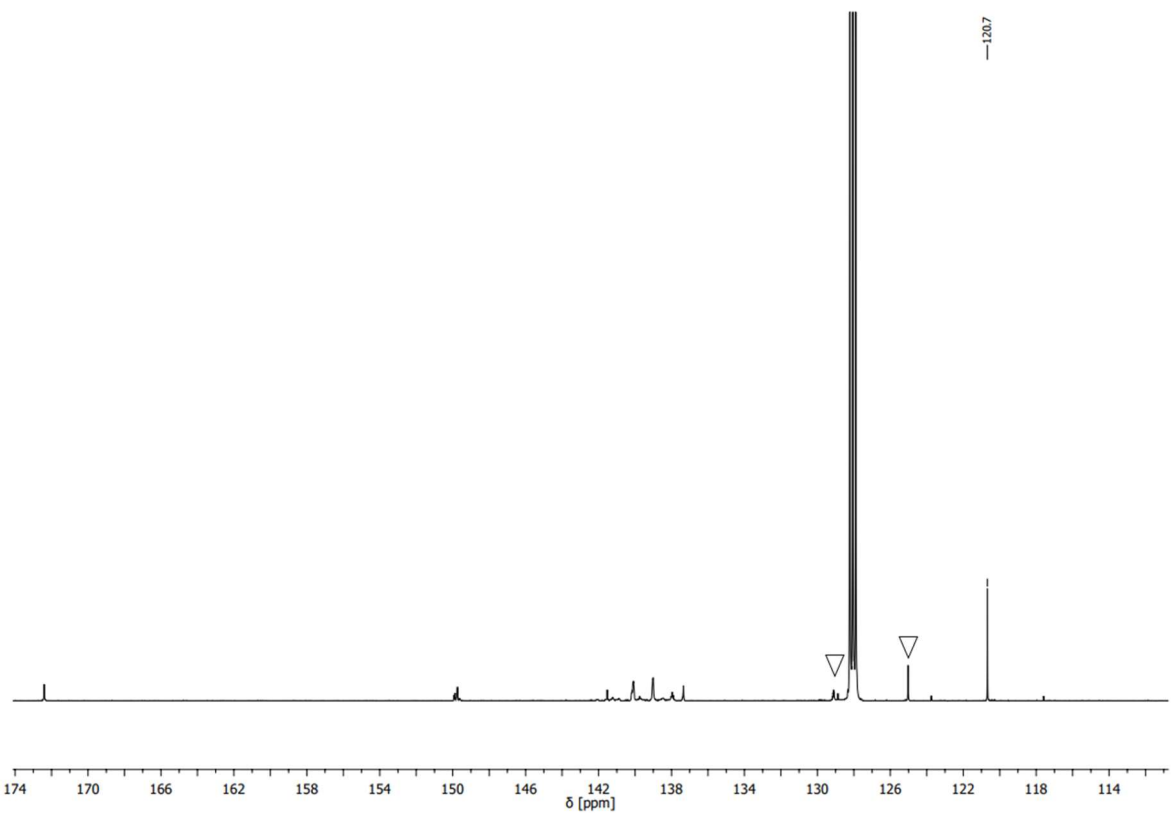


Fig. S23: $^{13}\text{C}\{^{19}\text{F}\}$ NMR of $^{17}\text{Fnac}_2\text{CuCO}$ in benzene- d_6 at room temperature with ^{19}F decoupling pulse at -60 ppm. Signals marked with ∇ belong to mesitylene.

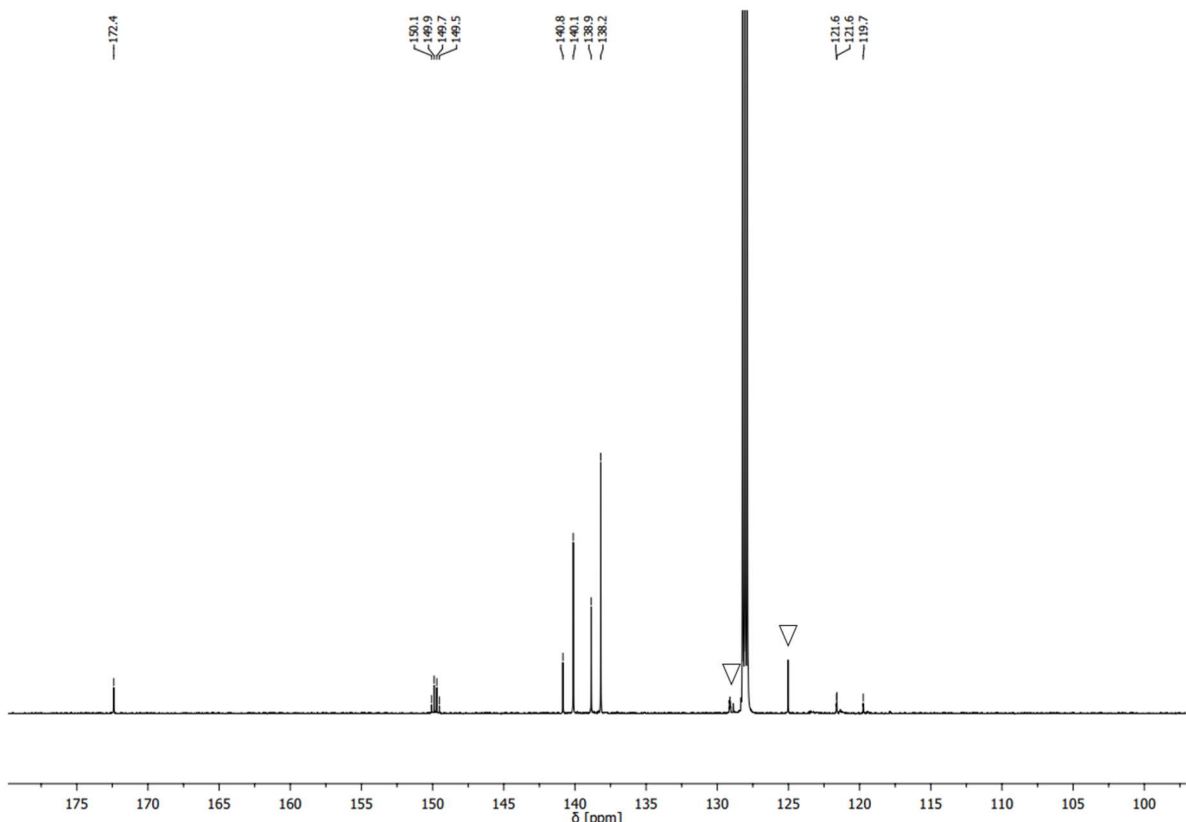


Fig. S24: $^{13}\text{C}\{^{19}\text{F}\}$ NMR of $^{17}\text{Fnac}_2\text{CuCO}$ in benzene- d_6 at room temperature with ^{19}F decoupling pulse at -110 ppm. Signals marked with ∇ belong to mesitylene.

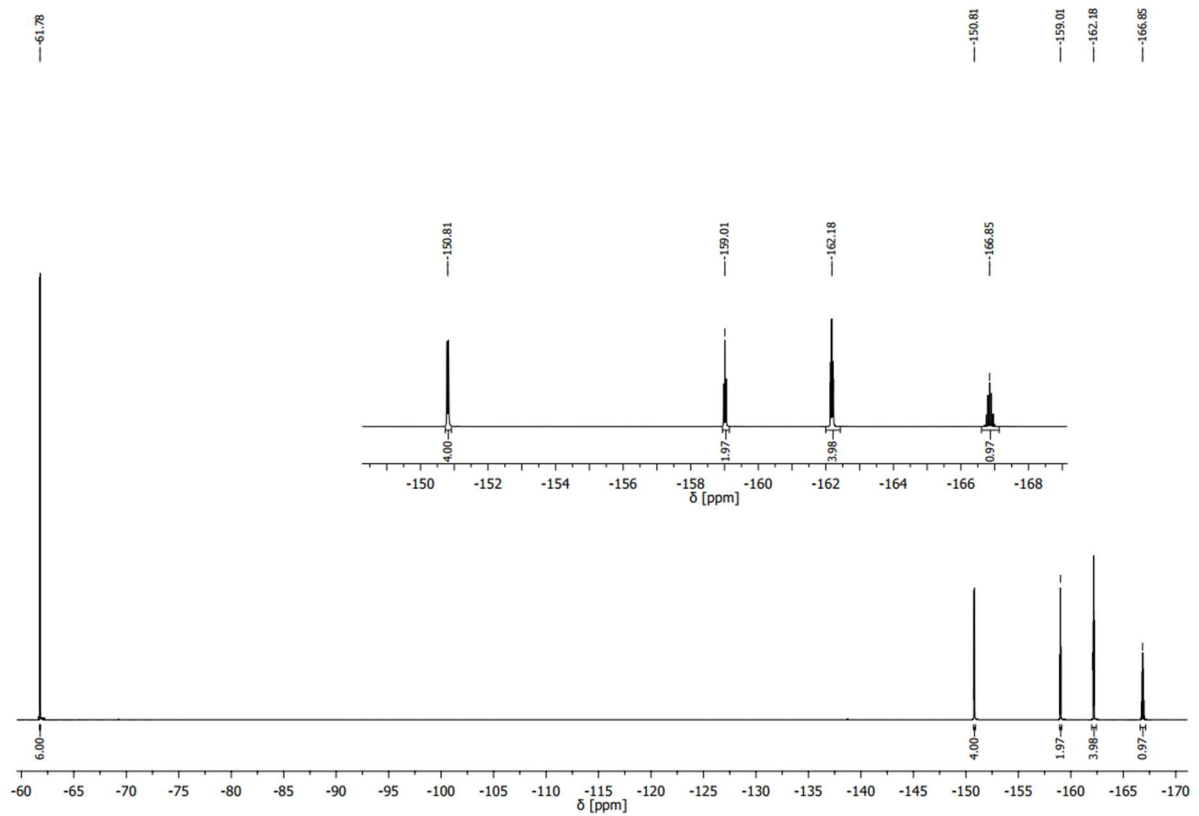


Fig. S25: ^{19}F NMR spectrum of $^{17}\text{Fnac}_2\text{CuCO}$ in benzene- d_6 at room temperature.

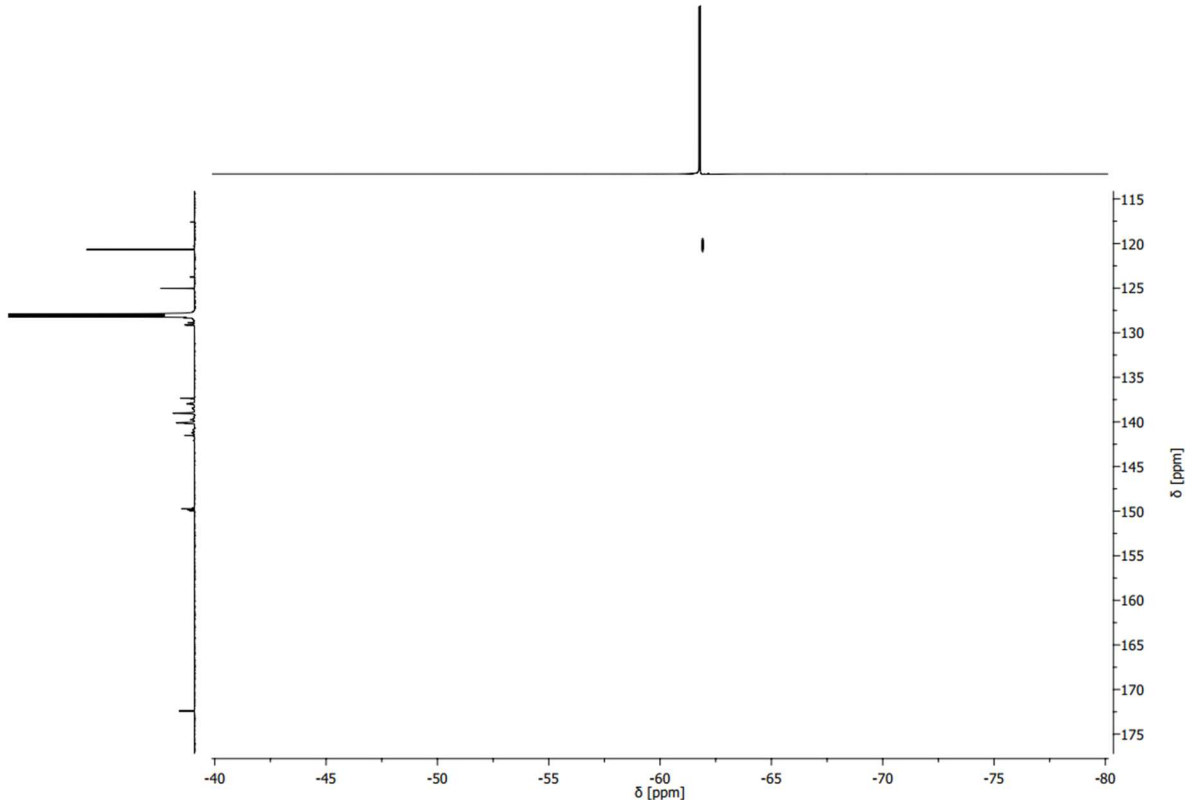


Fig. S26: $^{13}\text{C}-^{19}\text{F}$ HMQC NMR of $^{17}\text{Fnac}_2\text{CuCO}$ in benzene- d_6 at room temperature.

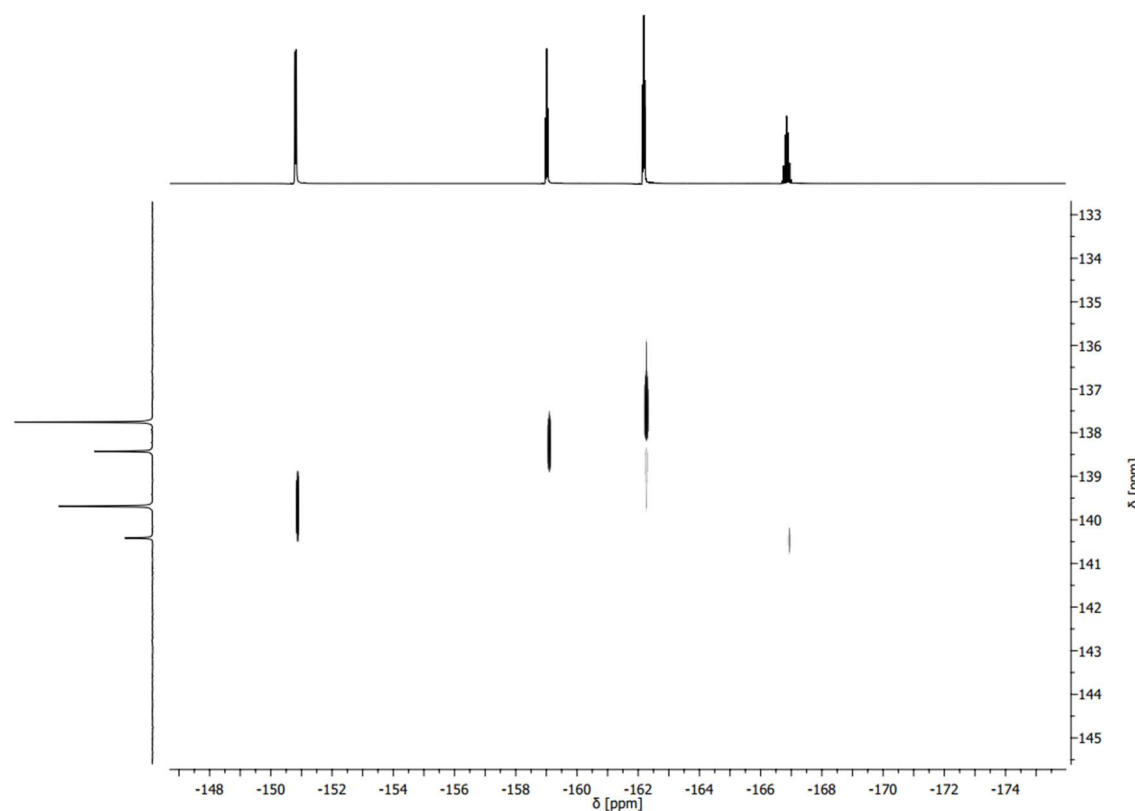


Fig. S27: ^{13}C - ^{19}F HMQC NMR of $^{17}\text{Fnac}_2\text{CuCO}$ in benzene- d_6 at room temperature.

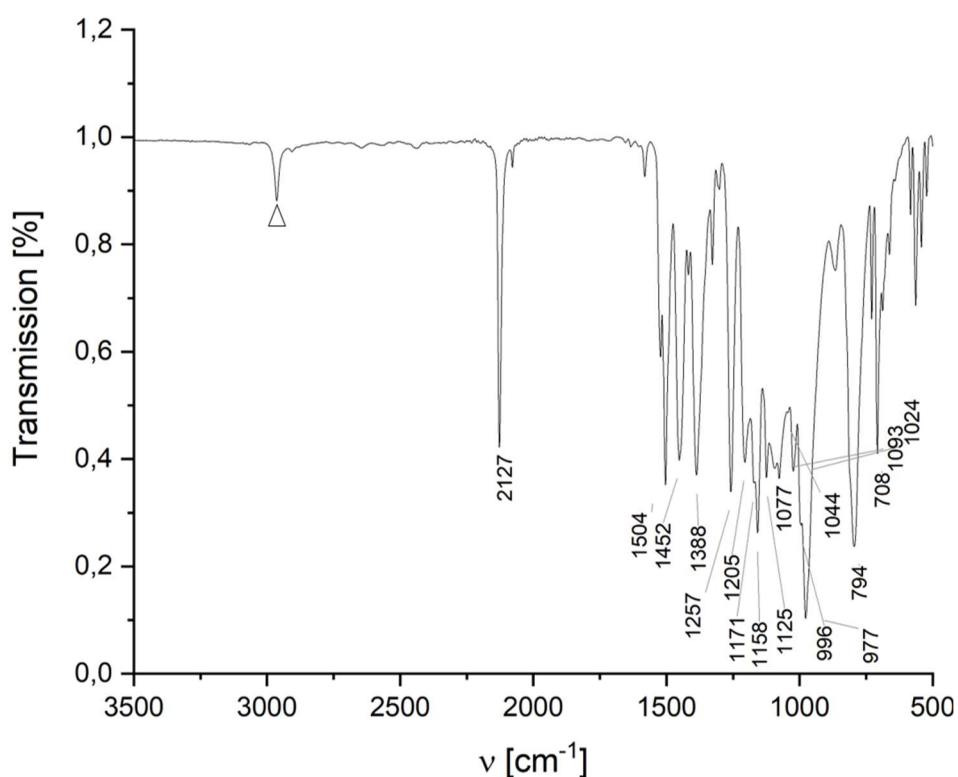


Fig. S28: ATR-IR spectrum of $^{17}\text{Fnac}_2\text{CuCO}$. The peak marked with ∇ belongs to n-hexane.

IV. Crystallographic details

Table S2: Crystallographic data of compounds **3** and **4**.

Identification code	3 (kh_v089_2m)	4 (kh_v092_2m)
Empirical formula	C ₂₃ H ₆ CuF ₁₇ N ₂	C ₁₈ CuF ₁₇ N ₂ O
<i>M</i>	696.84	646.74
Crystal size [mm]	0.388 × 0.270 × 0.088	0.360 × 0.122 × 0.105
<i>T</i> [K]	100(2)	100(2)
Crystal system	monoclinic	triclinic
Space group	<i>P</i> 2 ₁ / <i>n</i>	<i>P</i> -1
<i>a</i> [Å]	12.2119(18)	5.2839(8)
<i>b</i> [Å]	20.738(3)	9.5521(14)
<i>c</i> [Å]	18.601(3)	20.684(3)
α [°]	90	82.526(7)
β [°]	102.689(4)	83.221(7)
γ [°]	90	76.884(7)
<i>V</i> [Å ³]	4595.6(12)	1003.9(3)
<i>Z</i>	8	2
<i>D</i> _{calc} [g·cm ⁻³]	2.014	2.140
μ [mm ⁻¹]	2.847 Cu <i>K</i> _α	1.262 Mo <i>K</i> _α
Transmissions	0.75/0.54	0.75/0.59
<i>F</i> (000)	2720	624
Index ranges	-12 ≤ <i>h</i> ≤ 15 -26 ≤ <i>k</i> ≤ 26 -23 ≤ <i>l</i> ≤ 23	-7 ≤ <i>h</i> ≤ 7 -13 ≤ <i>k</i> ≤ 13 -28 ≤ <i>l</i> ≤ 29
θ_{max} [°]	80.719	30.888
Reflections collected	144722	34292
Independent reflections	10029	6192
<i>R</i> _{int}	0.0503	0.0425
Refined parameters	775	389
<i>R</i> ₁ [<i>I</i> > 2σ(<i>I</i>)]	0.0300	0.0329
<i>wR</i> ₂ [all data]	0.0834	0.0899
GooF	1.057	1.086
Δ <i>ρ</i> _{final} (max/min) [e·Å ⁻³]	0.610/-0.587	0.586/-0.551

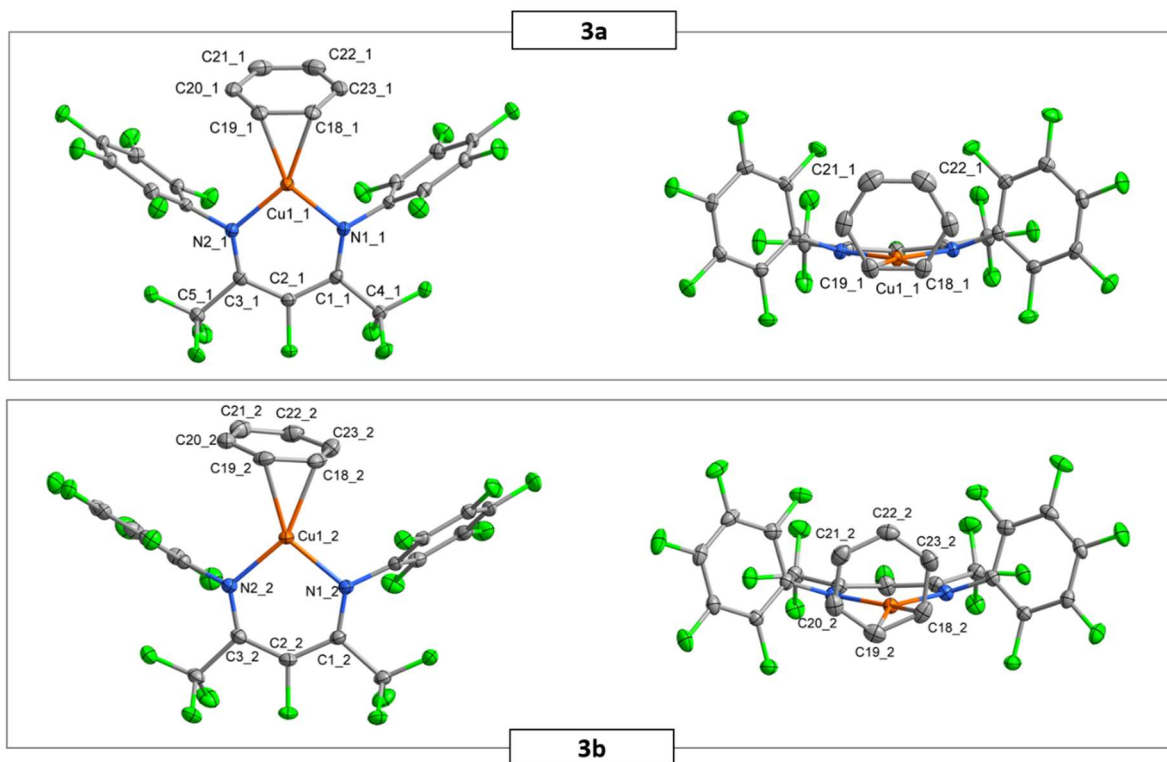


Fig S29: Molecular structure of $^{17}\text{Fnac}_2\text{CuC}_6\text{H}_6$ **3a** and **3b**; Displacement ellipsoids are drawn at the 50% probability level. Hydrogen atoms are omitted for clarity.

Table S3: Important bond lengths and angles for both molecules in the asymmetric unit in crystals of $^{17}\text{Fnac}_2\text{CuC}_6\text{H}_6$ (**3a** and **3b**)

	3a [$\text{\AA}/^\circ$]	3b [$\text{\AA}/^\circ$]
Cu-N1	1.9557(12)	1.9830(12)
Cu-N2	1.9539(12)	1.9652(12)
Cu-C18	2.1088(14)	2.1148(15)
Cu-C19	2.1092(15)	2.1831(15)
C18-C19	1.408(2)	1.400(2)
C19-C20	1.411(2)	1.398(2)
C20-C21	1.377(3)	1.370(2)
C21-C22	1.407(3)	1.397(2)
C22-C23	1.371(3)	1.380(2)
C23-C18	1.411(2)	1.426(2)
N1-Cu-N2	98.06(5)	98.99(5)

VI. Cyclic voltammetry

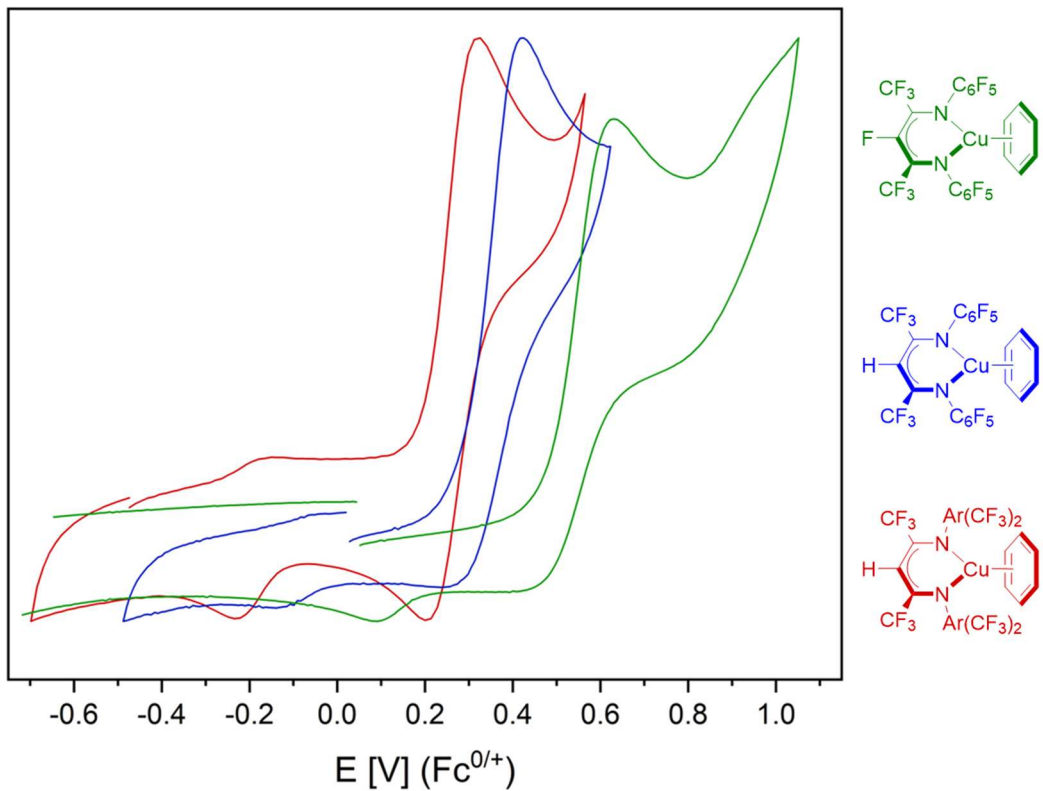


Fig S30: Overlay of cyclic voltammograms for LCuC_6H_6 complexes ($\text{L} = {}^{16}\text{Fnac}_2, {}^{17}\text{Fnac}_2$ (**3**); DCM/*n*-Bu₄BAr^F vs $\text{Fc}^{0/+}$).

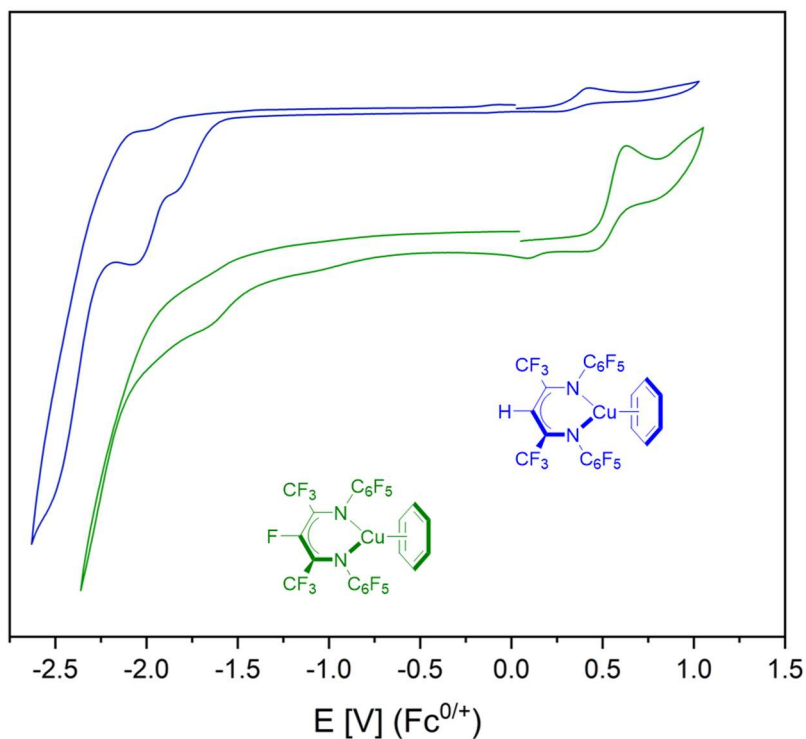


Fig S31: Overlay of cyclic voltammograms for LCuC_6H_6 complexes ($\text{L} = {}^{16}\text{Fnac}_2, {}^{17}\text{Fnac}_2$ (**3**); DCM/*n*-Bu₄BAr^F vs $\text{Fc}^{0/+}$) over a wide scan range.

Tabel S4: Cyclic voltammetry data in DCM/*n*-Bu₄BAr^F vs Fc^{0/+} with a scan rate of 100 mV/s for LCuC₆H₆ complexes (L = ¹⁶Fnac₂, ¹⁷Fnac₂ (**3**), ¹⁸Fnac₂).

	¹⁸ Fnac ₂ CuC ₆ H ₆		¹⁶ Fnac ₂ CuC ₆ H ₆		¹⁷ Fnac ₂ CuC ₆ H ₆
Potential [V]	Current	Potential [V]	Current	Potential	Current
-0.47394	-4.43E-09	0.02792	3.52E-07	0.05173	8.01E-07
-0.4599	-2.50E-09	0.03586	3.53E-07	0.05966	8.02E-07
-0.44586	-1.13E-09	0.04379	3.54E-07	0.0676	8.03E-07
-0.43182	2.14E-10	0.05173	3.55E-07	0.07553	8.04E-07
-0.41779	8.85E-10	0.05966	3.56E-07	0.08347	8.05E-07
-0.40375	2.04E-09	0.0676	3.56E-07	0.0914	8.05E-07
-0.38971	2.66E-09	0.07553	3.57E-07	0.09933	8.07E-07
-0.37567	3.42E-09	0.08347	3.57E-07	0.10727	8.06E-07
-0.36163	4.06E-09	0.0914	3.58E-07	0.1152	8.07E-07
-0.3476	5.00E-09	0.09933	3.58E-07	0.12314	8.08E-07
-0.33356	5.62E-09	0.10727	3.59E-07	0.13107	8.08E-07
-0.31952	6.32E-09	0.1152	3.59E-07	0.13901	8.09E-07
-0.30548	7.17E-09	0.12314	3.60E-07	0.14694	8.09E-07
-0.29144	7.66E-09	0.13107	3.61E-07	0.15488	8.10E-07
-0.2774	8.94E-09	0.13901	3.60E-07	0.16281	8.11E-07
-0.26337	9.64E-09	0.14694	3.62E-07	0.17075	8.11E-07
-0.24933	1.14E-08	0.15488	3.62E-07	0.17868	8.12E-07
-0.23529	1.28E-08	0.16281	3.63E-07	0.18661	8.12E-07
-0.22125	1.46E-08	0.17075	3.64E-07	0.19455	8.12E-07
-0.20721	1.66E-08	0.17868	3.65E-07	0.20248	8.13E-07
-0.19318	1.81E-08	0.18661	3.66E-07	0.21042	8.14E-07
-0.17914	1.92E-08	0.19455	3.68E-07	0.21835	8.14E-07
-0.1651	1.95E-08	0.20248	3.69E-07	0.22629	8.15E-07
-0.15106	2.01E-08	0.21042	3.71E-07	0.23422	8.15E-07
-0.13702	2.01E-08	0.21835	3.73E-07	0.24216	8.16E-07
-0.12299	2.00E-08	0.22629	3.75E-07	0.25009	8.16E-07
-0.10895	1.97E-08	0.23422	3.79E-07	0.25803	8.17E-07
-0.09491	1.95E-08	0.24216	3.83E-07	0.26596	8.18E-07
-0.08087	1.95E-08	0.25009	3.87E-07	0.2739	8.18E-07
-0.06683	1.93E-08	0.25803	3.92E-07	0.28183	8.19E-07
-0.0528	1.94E-08	0.26596	3.98E-07	0.28976	8.20E-07
-0.03876	1.91E-08	0.2739	4.05E-07	0.2977	8.20E-07
-0.02472	1.93E-08	0.28183	4.13E-07	0.30563	8.21E-07
-0.01068	1.92E-08	0.28976	4.22E-07	0.31357	8.22E-07
0.00336	1.92E-08	0.2977	4.32E-07	0.3215	8.22E-07
0.01739	1.93E-08	0.30563	4.44E-07	0.32944	8.24E-07
0.03143	1.93E-08	0.31357	4.57E-07	0.33737	8.24E-07
0.04547	1.95E-08	0.3215	4.73E-07	0.34531	8.25E-07
0.05951	1.94E-08	0.32944	4.90E-07	0.35324	8.26E-07
0.07355	1.99E-08	0.33737	5.10E-07	0.36118	8.28E-07
0.08759	1.99E-08	0.34531	5.33E-07	0.36911	8.29E-07

0.10162	2.07E-08	0.35324	5.56E-07	0.37704	8.30E-07
0.11566	2.08E-08	0.36118	5.80E-07	0.38498	8.32E-07
0.1297	2.18E-08	0.36911	6.06E-07	0.39291	8.34E-07
0.14374	2.40E-08	0.37704	6.26E-07	0.40085	8.36E-07
0.15778	2.62E-08	0.38498	6.47E-07	0.40878	8.38E-07
0.17181	3.06E-08	0.39291	6.62E-07	0.41672	8.41E-07
0.18585	3.71E-08	0.40085	6.73E-07	0.42465	8.44E-07
0.19989	4.74E-08	0.40878	6.80E-07	0.43259	8.49E-07
0.21393	6.23E-08	0.41672	6.84E-07	0.44052	8.53E-07
0.22797	8.39E-08	0.42465	6.84E-07	0.44846	8.59E-07
0.242	1.12E-07	0.43259	6.82E-07	0.45639	8.65E-07
0.25604	1.43E-07	0.44052	6.79E-07	0.46432	8.72E-07
0.27008	1.75E-07	0.44846	6.75E-07	0.47226	8.82E-07
0.28412	2.00E-07	0.45639	6.71E-07	0.48019	8.92E-07
0.29816	2.17E-07	0.46432	6.65E-07	0.48813	9.05E-07
0.31219	2.24E-07	0.47226	6.60E-07	0.49606	9.21E-07
0.32623	2.25E-07	0.48019	6.56E-07	0.504	9.39E-07
0.34027	2.21E-07	0.48813	6.50E-07	0.51193	9.60E-07
0.35431	2.15E-07	0.49606	6.46E-07	0.51987	9.85E-07
0.36835	2.09E-07	0.504	6.42E-07	0.5278	1.01E-06
0.38239	2.02E-07	0.51193	6.38E-07	0.53574	1.04E-06
0.39642	1.96E-07	0.51987	6.34E-07	0.54367	1.07E-06
0.41046	1.91E-07	0.5278	6.31E-07	0.55161	1.11E-06
0.4245	1.86E-07	0.53574	6.28E-07	0.55954	1.14E-06
0.43854	1.83E-07	0.54367	6.26E-07	0.56747	1.17E-06
0.45258	1.79E-07	0.55161	6.23E-07	0.57541	1.20E-06
0.46661	1.77E-07	0.55954	6.21E-07	0.58334	1.23E-06
0.48065	1.75E-07	0.56747	6.19E-07	0.59128	1.24E-06
0.49469	1.75E-07	0.57541	6.17E-07	0.59921	1.26E-06
0.50873	1.76E-07	0.58334	6.16E-07	0.60715	1.27E-06
0.52277	1.78E-07	0.59128	6.15E-07	0.61508	1.28E-06
0.5368	1.82E-07	0.59921	6.14E-07	0.62302	1.28E-06
0.55084	1.88E-07	0.60715	6.13E-07	0.63095	1.28E-06
0.56488	1.98E-07	0.61508	6.12E-07	0.63889	1.28E-06
0.55084	1.73E-07	0.62302	6.12E-07	0.64682	1.28E-06
0.5368	1.57E-07	0.61508	5.97E-07	0.65475	1.28E-06
0.52277	1.45E-07	0.60715	5.86E-07	0.66269	1.27E-06
0.50873	1.36E-07	0.59921	5.76E-07	0.67062	1.27E-06
0.49469	1.30E-07	0.59128	5.68E-07	0.67856	1.26E-06
0.48065	1.24E-07	0.58334	5.60E-07	0.68649	1.26E-06
0.46661	1.20E-07	0.57541	5.54E-07	0.69443	1.25E-06
0.45258	1.16E-07	0.56747	5.48E-07	0.70236	1.25E-06
0.43854	1.13E-07	0.55954	5.42E-07	0.7103	1.24E-06
0.4245	1.10E-07	0.55161	5.38E-07	0.71823	1.24E-06
0.41046	1.07E-07	0.54367	5.33E-07	0.72617	1.23E-06
0.39642	1.03E-07	0.53574	5.28E-07	0.7341	1.23E-06
0.38239	1.00E-07	0.5278	5.24E-07	0.74203	1.23E-06
0.36835	9.54E-08	0.51987	5.20E-07	0.74997	1.23E-06

0.35431	8.96E-08	0.51193	5.17E-07	0.7579	1.22E-06
0.34027	8.21E-08	0.504	5.13E-07	0.76584	1.22E-06
0.32623	7.19E-08	0.49606	5.09E-07	0.77377	1.22E-06
0.31219	5.81E-08	0.48813	5.06E-07	0.78171	1.22E-06
0.29816	4.07E-08	0.48019	5.02E-07	0.78964	1.22E-06
0.28412	1.95E-08	0.47226	4.98E-07	0.79758	1.22E-06
0.27008	-2.78E-09	0.46432	4.93E-07	0.80551	1.22E-06
0.25604	-2.49E-08	0.45639	4.89E-07	0.81345	1.22E-06
0.242	-4.20E-08	0.44846	4.84E-07	0.82138	1.22E-06
0.22797	-5.33E-08	0.44052	4.79E-07	0.82932	1.22E-06
0.21393	-5.86E-08	0.43259	4.73E-07	0.83725	1.22E-06
0.19989	-5.95E-08	0.42465	4.66E-07	0.84518	1.23E-06
0.18585	-5.79E-08	0.41672	4.59E-07	0.85312	1.23E-06
0.17181	-5.51E-08	0.40878	4.51E-07	0.86105	1.24E-06
0.15778	-5.22E-08	0.40085	4.42E-07	0.86899	1.24E-06
0.14374	-4.92E-08	0.39291	4.34E-07	0.87692	1.25E-06
0.1297	-4.66E-08	0.38498	4.22E-07	0.88486	1.25E-06
0.11566	-4.41E-08	0.37704	4.12E-07	0.89279	1.26E-06
0.10162	-4.21E-08	0.36911	4.01E-07	0.90073	1.27E-06
0.08759	-4.02E-08	0.36118	3.91E-07	0.90866	1.28E-06
0.07355	-3.87E-08	0.35324	3.80E-07	0.9166	1.28E-06
0.05951	-3.75E-08	0.34531	3.70E-07	0.92453	1.29E-06
0.04547	-3.64E-08	0.33737	3.61E-07	0.93246	1.30E-06
0.03143	-3.55E-08	0.32944	3.53E-07	0.9404	1.30E-06
0.01739	-3.45E-08	0.3215	3.46E-07	0.94833	1.31E-06
0.00336	-3.39E-08	0.31357	3.39E-07	0.95627	1.31E-06
-0.01068	-3.33E-08	0.30563	3.35E-07	0.9642	1.32E-06
-0.02472	-3.29E-08	0.2977	3.30E-07	0.97214	1.33E-06
-0.03876	-3.24E-08	0.28976	3.28E-07	0.98007	1.33E-06
-0.0528	-3.21E-08	0.28183	3.26E-07	0.98801	1.34E-06
-0.06683	-3.20E-08	0.2739	3.24E-07	0.99594	1.34E-06
-0.08087	-3.21E-08	0.26596	3.23E-07	1.00388	1.35E-06
-0.09491	-3.25E-08	0.25803	3.23E-07	1.01181	1.35E-06
-0.10895	-3.33E-08	0.25009	3.22E-07	1.01974	1.35E-06
-0.12299	-3.45E-08	0.24216	3.22E-07	1.02768	1.36E-06
-0.13702	-3.66E-08	0.23422	3.22E-07	1.03561	1.36E-06
-0.15106	-3.98E-08	0.22629	3.22E-07	1.04355	1.37E-06
-0.1651	-4.39E-08	0.21835	3.22E-07	1.05148	1.38E-06
-0.17914	-4.87E-08	0.21042	3.22E-07	1.04355	1.34E-06
-0.19318	-5.33E-08	0.20248	3.23E-07	1.03561	1.31E-06
-0.20721	-5.65E-08	0.19455	3.23E-07	1.02768	1.29E-06
-0.22125	-5.83E-08	0.18661	3.23E-07	1.01974	1.27E-06
-0.23529	-5.87E-08	0.17868	3.23E-07	1.01181	1.25E-06
-0.24933	-5.78E-08	0.17075	3.23E-07	1.00388	1.23E-06
-0.26337	-5.65E-08	0.16281	3.24E-07	0.99594	1.22E-06
-0.2774	-5.49E-08	0.15488	3.24E-07	0.98801	1.20E-06
-0.29144	-5.34E-08	0.14694	3.24E-07	0.98007	1.19E-06
-0.30548	-5.18E-08	0.13901	3.24E-07	0.97214	1.18E-06

-0.31952	-5.08E-08	0.13107	3.24E-07	0.9642	1.17E-06
-0.33356	-4.96E-08	0.12314	3.24E-07	0.95627	1.16E-06
-0.3476	-4.89E-08	0.1152	3.25E-07	0.94833	1.15E-06
-0.36163	-4.83E-08	0.10727	3.24E-07	0.9404	1.13E-06
-0.37567	-4.79E-08	0.09933	3.24E-07	0.93246	1.12E-06
-0.38971	-4.79E-08	0.0914	3.24E-07	0.92453	1.12E-06
-0.40375	-4.76E-08	0.08347	3.24E-07	0.9166	1.11E-06
-0.41779	-4.77E-08	0.07553	3.24E-07	0.90866	1.10E-06
-0.43182	-4.80E-08	0.0676	3.24E-07	0.90073	1.09E-06
-0.44586	-4.86E-08	0.05966	3.25E-07	0.89279	1.08E-06
-0.4599	-4.84E-08	0.05173	3.24E-07	0.88486	1.07E-06
-0.47394	-4.90E-08	0.04379	3.24E-07	0.87692	1.06E-06
-0.48798	-4.94E-08	0.03586	3.24E-07	0.86899	1.06E-06
-0.50201	-4.98E-08	0.02792	3.24E-07	0.86105	1.05E-06
-0.51605	-5.04E-08	0.01999	3.24E-07	0.85312	1.04E-06
-0.53009	-5.10E-08	0.01205	3.24E-07	0.84518	1.04E-06
-0.54413	-5.13E-08	0.00412	3.23E-07	0.83725	1.03E-06
-0.55817	-5.19E-08	-0.00381	3.23E-07	0.82932	1.03E-06
-0.5722	-5.26E-08	-0.01175	3.23E-07	0.82138	1.02E-06
-0.58624	-5.30E-08	-0.01968	3.22E-07	0.81345	1.02E-06
-0.60028	-5.37E-08	-0.02762	3.21E-07	0.80551	1.02E-06
-0.61432	-5.43E-08	-0.03555	3.21E-07	0.79758	1.01E-06
-0.62836	-5.52E-08	-0.04349	3.20E-07	0.78964	1.01E-06
-0.6424	-5.58E-08	-0.05142	3.19E-07	0.78171	1.01E-06
-0.65643	-5.69E-08	-0.05936	3.17E-07	0.77377	1.01E-06
-0.67047	-5.77E-08	-0.06729	3.16E-07	0.76584	1.00E-06
-0.68451	-5.87E-08	-0.07523	3.14E-07	0.7579	1.00E-06
-0.69855	-5.99E-08	-0.08316	3.13E-07	0.74997	1.00E-06
-0.68451	-4.33E-08	-0.09109	3.13E-07	0.74203	9.98E-07
-0.67047	-3.36E-08	-0.09903	3.10E-07	0.7341	9.96E-07
-0.65643	-2.67E-08	-0.10696	3.11E-07	0.72617	9.95E-07
-0.6424	-2.19E-08	-0.1149	3.09E-07	0.71823	9.93E-07
-0.62836	-1.78E-08	-0.12283	3.09E-07	0.7103	9.91E-07
-0.61432	-1.50E-08	-0.13077	3.09E-07	0.70236	9.89E-07
-0.60028	-1.22E-08	-0.1387	3.08E-07	0.69443	9.88E-07
-0.58624	-1.01E-08	-0.14664	3.08E-07	0.68649	9.86E-07
-0.5722	-8.36E-09	-0.15457	3.09E-07	0.67856	9.83E-07
-0.55817	-6.65E-09	-0.16251	3.09E-07	0.67062	9.81E-07
-0.54413	-5.31E-09	-0.17044	3.09E-07	0.66269	9.78E-07
-0.53009	-3.88E-09	-0.17838	3.10E-07	0.65475	9.75E-07
-0.51605	-2.75E-09	-0.18631	3.09E-07	0.64682	9.71E-07
-0.50201	-1.65E-09	-0.19424	3.10E-07	0.63889	9.67E-07
-0.48798	-6.71E-10	-0.20218	3.10E-07	0.63095	9.63E-07
-0.47394	2.75E-10	-0.21011	3.10E-07	0.62302	9.55E-07
		-0.21805	3.10E-07	0.61508	9.50E-07
		-0.22598	3.10E-07	0.60715	9.42E-07
		-0.23392	3.10E-07	0.59921	9.33E-07
		-0.24185	3.10E-07	0.59128	9.23E-07

-0.24979	3.11E-07	0.58334	9.12E-07
-0.25772	3.11E-07	0.57541	8.99E-07
-0.26566	3.11E-07	0.56747	8.86E-07
-0.27359	3.11E-07	0.55954	8.72E-07
-0.28152	3.10E-07	0.55161	8.58E-07
-0.28946	3.10E-07	0.54367	8.44E-07
-0.29739	3.10E-07	0.53574	8.30E-07
-0.30533	3.10E-07	0.5278	8.18E-07
-0.31326	3.09E-07	0.51987	8.06E-07
-0.3212	3.10E-07	0.51193	7.95E-07
-0.32913	3.10E-07	0.504	7.86E-07
-0.33707	3.08E-07	0.49606	7.78E-07
-0.345	3.09E-07	0.48813	7.71E-07
-0.35294	3.08E-07	0.48019	7.66E-07
-0.36087	3.08E-07	0.47226	7.62E-07
-0.3688	3.08E-07	0.46432	7.58E-07
-0.37674	3.07E-07	0.45639	7.55E-07
-0.38467	3.07E-07	0.44846	7.53E-07
-0.39261	3.06E-07	0.44052	7.52E-07
-0.40054	3.06E-07	0.43259	7.51E-07
-0.40848	3.05E-07	0.42465	7.50E-07
-0.41641	3.05E-07	0.41672	7.49E-07
-0.42435	3.04E-07	0.40878	7.49E-07
-0.43228	3.04E-07	0.40085	7.49E-07
-0.44022	3.04E-07	0.39291	7.48E-07
-0.44815	3.03E-07	0.38498	7.48E-07
-0.45609	3.02E-07	0.37704	7.48E-07
-0.46402	3.01E-07	0.36911	7.48E-07
-0.47195	3.01E-07	0.36118	7.48E-07
-0.47989	3.00E-07	0.35324	7.48E-07
-0.48782	3.00E-07	0.34531	7.48E-07
-0.47989	3.10E-07	0.33737	7.48E-07
-0.47195	3.17E-07	0.32944	7.48E-07
-0.46402	3.22E-07	0.3215	7.48E-07
-0.45609	3.26E-07	0.31357	7.48E-07
-0.44815	3.30E-07	0.30563	7.48E-07
-0.44022	3.33E-07	0.2977	7.49E-07
-0.43228	3.35E-07	0.28976	7.48E-07
-0.42435	3.37E-07	0.28183	7.48E-07
-0.41641	3.40E-07	0.2739	7.48E-07
-0.40848	3.42E-07	0.26596	7.48E-07
-0.40054	3.43E-07	0.25803	7.48E-07
-0.39261	3.45E-07	0.25009	7.48E-07
-0.38467	3.46E-07	0.24216	7.48E-07
-0.37674	3.47E-07	0.23422	7.47E-07
-0.3688	3.48E-07	0.22629	7.47E-07
-0.36087	3.49E-07	0.21835	7.46E-07
-0.35294	3.49E-07	0.21042	7.45E-07

-0.345	3.50E-07	0.20248	7.44E-07
-0.33707	3.51E-07	0.19455	7.43E-07
-0.32913	3.51E-07	0.18661	7.42E-07
-0.3212	3.52E-07	0.17868	7.40E-07
-0.31326	3.52E-07	0.17075	7.39E-07
-0.30533	3.53E-07	0.16281	7.35E-07
-0.29739	3.54E-07	0.15488	7.33E-07
-0.28946	3.54E-07	0.14694	7.30E-07
-0.28152	3.55E-07	0.13901	7.27E-07
-0.27359	3.55E-07	0.13107	7.24E-07
-0.26566	3.56E-07	0.12314	7.21E-07
-0.25772	3.56E-07	0.1152	7.19E-07
-0.24979	3.57E-07	0.10727	7.17E-07
-0.24185	3.57E-07	0.09933	7.16E-07
-0.23392	3.58E-07	0.0914	7.15E-07
-0.22598	3.58E-07	0.08347	7.15E-07
-0.21805	3.59E-07	0.07553	7.16E-07
-0.21011	3.59E-07	0.0676	7.17E-07
-0.20218	3.59E-07	0.05966	7.18E-07
-0.19424	3.60E-07	0.05173	7.19E-07
-0.18631	3.60E-07	0.04379	7.20E-07
-0.17838	3.61E-07	0.03586	7.21E-07
-0.17044	3.61E-07	0.02792	7.23E-07
-0.16251	3.61E-07	0.01999	7.24E-07
-0.15457	3.63E-07	0.01205	7.25E-07
-0.14664	3.63E-07	0.00412	7.26E-07
-0.1387	3.63E-07	-0.00381	7.27E-07
-0.13077	3.64E-07	-0.01175	7.28E-07
-0.12283	3.64E-07	-0.01968	7.29E-07
-0.1149	3.65E-07	-0.02762	7.30E-07
-0.10696	3.65E-07	-0.03555	7.31E-07
-0.09903	3.67E-07	-0.04349	7.31E-07
-0.09109	3.67E-07	-0.05142	7.32E-07
-0.08316	3.68E-07	-0.05936	7.34E-07
-0.07523	3.68E-07	-0.06729	7.33E-07
-0.06729	3.69E-07	-0.07523	7.34E-07
-0.05936	3.70E-07	-0.08316	7.35E-07
-0.05142	3.70E-07	-0.09109	7.36E-07
-0.04349	3.70E-07	-0.09903	7.36E-07
-0.03555	3.70E-07	-0.10696	7.36E-07
-0.02762	3.70E-07	-0.1149	7.37E-07
-0.01968	3.70E-07	-0.12283	7.37E-07
-0.01175	3.71E-07	-0.13077	7.37E-07
-0.00381	3.71E-07	-0.1387	7.38E-07
0.00412	3.71E-07	-0.14664	7.39E-07
0.01205	3.71E-07	-0.15457	7.39E-07
0.01999	3.71E-07	-0.16251	7.39E-07
		-0.17044	7.39E-07

-0.17838	7.40E-07
-0.18631	7.40E-07
-0.19424	7.40E-07
-0.20218	7.41E-07
-0.21011	7.41E-07
-0.21805	7.41E-07
-0.22598	7.41E-07
-0.23392	7.42E-07
-0.24185	7.42E-07
-0.24979	7.42E-07
-0.25772	7.42E-07
-0.26566	7.42E-07
-0.27359	7.43E-07
-0.28152	7.43E-07
-0.28946	7.44E-07
-0.29739	7.42E-07
-0.30533	7.43E-07
-0.31326	7.43E-07
-0.3212	7.43E-07
-0.32913	7.43E-07
-0.33707	7.43E-07
-0.345	7.43E-07
-0.35294	7.43E-07
-0.36087	7.43E-07
-0.3688	7.43E-07
-0.37674	7.43E-07
-0.38467	7.43E-07
-0.39261	7.43E-07
-0.40054	7.43E-07
-0.40848	7.43E-07
-0.41641	7.43E-07
-0.42435	7.43E-07
-0.43228	7.42E-07
-0.44022	7.42E-07
-0.44815	7.42E-07
-0.45609	7.42E-07
-0.46402	7.42E-07
-0.47195	7.41E-07
-0.47989	7.41E-07
-0.48782	7.41E-07
-0.49576	7.41E-07
-0.50369	7.40E-07
-0.51163	7.40E-07
-0.51956	7.40E-07
-0.5275	7.38E-07
-0.53543	7.39E-07
-0.54337	7.38E-07
-0.5513	7.38E-07

-0.55923	7.37E-07
-0.56717	7.37E-07
-0.5751	7.36E-07
-0.58304	7.36E-07
-0.59097	7.35E-07
-0.59891	7.35E-07
-0.60684	7.34E-07
-0.61478	7.33E-07
-0.62271	7.33E-07
-0.63065	7.32E-07
-0.63858	7.31E-07
-0.64651	7.30E-07
-0.65445	7.30E-07
-0.66238	7.29E-07
-0.67032	7.28E-07
-0.67825	7.27E-07
-0.68619	7.26E-07
-0.69412	7.25E-07
-0.70206	7.24E-07
-0.70999	7.23E-07
-0.71793	7.22E-07

VII. Computational details

The geometric parameters of model anions L^- were fully optimized in the gas phase at the B3LYP/6-31G(d,p) theoretical level using Gaussian16 without constrictions for Mesnac₂⁻, ¹⁶Fnac₂⁻ and with constrictions to C₆F₅ torsion angles for ¹⁷Fnac₂⁻. The stationary points were characterized as true minima on the potential energy surface by vibrational analysis (the number of imaginary frequencies (NImag) was equal to zero) and the structures obtained were used for the subsequent calculations. The natural bond orbital analysis (NBO)^[2] was performed at the B3LYP/6-31G(d,p)^[3-6] theoretical level as implemented in Gaussian16.^[7,8]

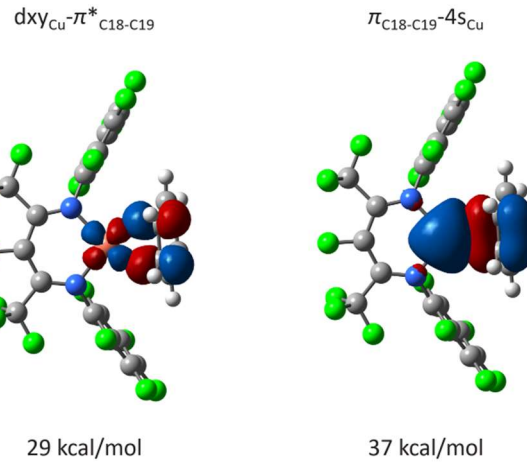


Fig S32: Graphical illustration of NBO interactions with the obtained interaction energies for ¹⁷Fnac₂CuC₆H₆.

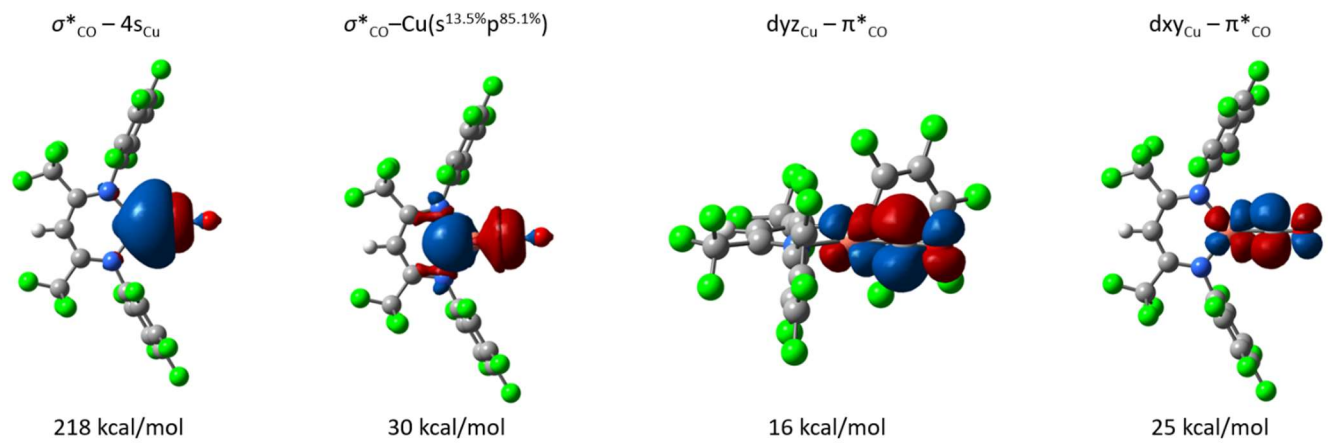


Fig S33: Graphical illustration of NBO interactions with the obtained interaction energies for ¹⁶Fnac₂CuCO.

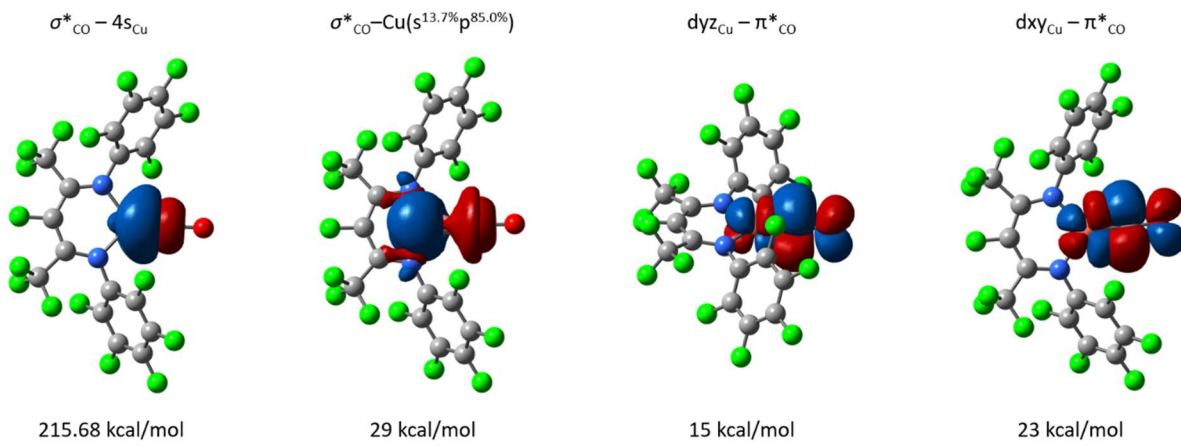


Fig S34: Graphical illustration of NBO interactions with the obtained interaction energies for $^{17}\text{Fnac}_2\text{CuCO}$.

Table S5: Cartesian coordinates (x,y,z) for the optimized geometry of model anion Mesnac₂⁻.

C	-2.740953	-0.016015	0.000273
C	-3.365691	-0.396758	-1.219261
C	-4.577846	-1.088876	-1.194478
H	-5.040336	-1.365834	-2.142566
C	-5.212353	-1.443249	0.001641
C	-4.57872	-1.085081	1.196995
H	-5.041925	-1.359072	2.145586
C	-3.366519	-0.392843	1.220492
C	-2.688091	-0.051616	2.523473
H	-2.707466	1.026134	2.731366
H	-1.629511	-0.329612	2.48056
H	-3.164894	-0.563443	3.366904
C	-2.686244	-0.05968	-2.522791
H	-3.162669	-0.573832	-3.365016
H	-1.627792	-0.337931	-2.478312
H	-2.705046	1.017455	-2.733861
C	-6.504831	-2.227431	0.002322
H	-7.116807	-1.995275	-0.877218
H	-7.107319	-2.008367	0.891616
H	-6.334952	-3.314129	-0.006812
C	-1.277042	1.865095	-0.00232
C	-2.469233	2.828731	-0.004073
H	-3.104214	2.659466	-0.881783
H	-2.151394	3.87489	-0.005362
H	-3.10492	2.661811	0.873572
C	0.001509	2.475075	-0.003118
C	1.279174	1.863223	-0.002372

C	2.472873	2.824965	-0.004015
H	3.108489	2.656465	0.873385
H	2.156858	3.871667	-0.004775
H	3.107329	2.654904	-0.88201
C	2.740979	-0.018796	0.000177
C	3.362894	-0.401759	1.220405
C	4.571494	-1.100302	1.197142
H	5.029095	-1.383424	2.145723
C	5.206595	-1.456337	0.001877
C	4.571016	-1.103907	-1.194294
H	5.028242	-1.389909	-2.142199
C	3.362473	-0.40546	-1.219182
C	2.677776	-0.076955	-2.522105
H	1.618857	-0.352256	-2.4709
H	3.149497	-0.598115	-3.362679
H	2.698292	0.99864	-2.740866
C	2.678737	-0.069338	2.522624
H	3.150204	-0.588728	3.364434
H	1.619586	-0.3439	2.472284
H	2.700206	1.006791	2.73867
C	6.533916	-2.179715	0.002612
H	7.388382	-1.486771	-0.005479
H	6.641094	-2.824663	-0.877335
H	6.646938	-2.811494	0.891282
N	-1.488734	0.568226	-0.000285
N	1.489077	0.566093	-0.000518
H	0.002313	3.560479	-0.004733

Table S6: Cartesian coordinates (x,y,z) for the optimized geometry of model anion $^{16}\text{Fnac}_2^-$.

F	-3.242908	2.33428	-1.045746
F	-3.263855	2.251452	1.127997
F	-2.154419	3.812721	0.109772
F	3.263869	2.251354	-1.128311
F	3.24292	2.334422	1.045419
F	2.154415	3.812733	-0.11026
F	-2.892991	-0.182829	-2.311859
F	-5.114723	-1.723076	-2.34664
F	-6.126091	-2.753819	-0.017495
F	-4.881979	-2.189067	2.357638
F	-2.660338	-0.648963	2.408289
F	2.660239	-0.649799	-2.408263
F	4.881874	-2.189869	-2.357183
F	6.126087	-2.753835	0.018097
F	5.114795	-1.722333	2.346933
F	2.893056	-0.182118	2.311738
N	-1.453661	0.265454	0.062861

N	1.453689	0.265468	-0.063149
C	-1.254173	1.556505	0.035954
C	0.000009	2.195689	-0.000148
C	1.254189	1.55652	-0.036243
C	-2.469567	2.497385	0.056456
C	2.469578	2.497405	-0.056799
C	-2.68017	-0.361294	0.049138
C	-3.355225	-0.671881	-1.148537
C	-4.500983	-1.459155	-1.176331
C	-5.018262	-1.985298	0.003497
C	-4.381026	-1.697651	1.20717
C	-3.23601	-0.909795	1.222337
C	2.680178	-0.361284	-0.049209
C	3.235961	-0.910211	-1.222242
C	4.380978	-1.698063	-1.206857
C	5.01826	-1.985315	-0.003115
C	4.501028	-1.45877	1.176555
C	3.355275	-0.671503	1.148546
H	0.000001	3.272543	-0.000158

Table S7: Cartesian coordinates (x,y,z) for the optimized geometry of model anion $^{17}\text{Fnac}_2^-$.

F	3.516719	1.688123	-0.940703
F	1.98229	3.023006	-1.637785
F	2.713598	3.180347	0.411326
F	0.034364	3.315155	-0.026231
F	-2.529446	3.116947	-0.820333
F	-3.593893	1.911316	0.631294
F	-2.137784	3.340746	1.31469
F	3.521675	0.605355	1.934071
F	5.837574	-0.792628	1.956669
F	6.32719	-2.704339	0.057967
F	4.435832	-3.213303	-1.863186
F	2.061024	-1.858585	-1.840515
F	-2.640452	-1.404685	2.450112
F	-4.93816	-2.797397	2.108482
F	-6.291535	-2.670996	-0.270093
F	-5.300674	-1.124328	-2.305504
F	-2.991011	0.248892	-1.966034
N	1.46658	0.033534	0.073196
N	-1.469281	0.081748	0.373737
C	1.271292	1.319087	-0.097012
C	0.016049	1.937821	0.071612
C	-1.262234	1.372356	0.255188
C	2.375357	2.306699	-0.561362
C	-2.382682	2.438539	0.337808
C	2.714482	-0.564711	0.029275
C	3.712059	-0.346162	1.000395
C	4.910445	-1.049348	1.013395

C	5.167533	-2.017265	0.045818
C	4.206359	-2.270967	-0.929178
C	3.01675	-1.555323	-0.928623
C	-2.759804	-0.504172	0.25169
C	-3.274257	-1.326634	1.268489
C	-4.455571	-2.040894	1.104161
C	-5.148973	-1.976622	-0.102151
C	-4.647276	-1.182967	-1.129304
C	-3.467343	-0.469372	-0.942964

Table S8: Cartesian coordinates (x,y,z) for the optimized geometry of $^{17}\text{Fnac}_2\text{CuC}_6\text{H}_6$.

Cu	-0.000009	-0.661784	-0.356327
F	2.451439	3.557223	1.105172
F	3.641612	2.379397	-0.269078
F	2.260464	3.831054	-1.053838
F	-2.451959	3.55699	1.104811
F	-3.641756	2.379214	-0.269853
F	-2.260538	3.831042	-1.054131
F	-0.000157	3.81744	0.097774
F	2.876959	0.462036	2.17276
F	5.228846	-0.879574	2.414256
F	6.357558	-2.065519	0.226486
F	5.106732	-1.908071	-2.200332
F	2.751721	-0.590217	-2.436421
F	-2.87708	0.462567	2.172474
F	-5.228861	-0.879174	2.414344
F	-6.357469	-2.065824	0.2269
F	-5.106664	-1.908929	-2.199959
F	-2.751787	-0.590921	-2.436429
N	1.479712	0.572388	-0.246323
N	-1.479819	0.572319	-0.246635
C	1.278832	1.881578	-0.116819
C	-0.000108	2.461781	-0.053008
C	-1.279005	1.881519	-0.117056
C	2.424171	2.922693	-0.077072
C	-2.424396	2.922574	-0.0775
C	2.762789	-0.010587	-0.139042
C	3.420762	-0.116129	1.091893
C	4.622888	-0.80213	1.225059
C	5.199266	-1.409883	0.110196
C	4.561304	-1.327973	-1.125975
C	3.359119	-0.634962	-1.237717
C	-2.762843	-0.010719	-0.139191
C	-3.420839	-0.115944	1.091771
C	-4.622908	-0.802012	1.225128
C	-5.199236	-1.410121	0.110428
C	-4.561279	-1.328508	-1.125752
C	-3.359154	-0.635425	-1.237692

C	-0.714381	-2.533534	-0.684259
H	-1.251629	-2.408323	-1.620899
C	-1.402895	-3.107555	0.423533
H	-2.48666	-3.161475	0.402985
C	-0.707065	-3.602182	1.506609
H	-1.244185	-4.028186	2.348403
C	0.708117	-3.602184	1.506348
H	1.245545	-4.028206	2.347936
C	1.403531	-3.107522	0.423029
H	2.487289	-3.161387	0.402092
C	0.714599	-2.53347	-0.684488
H	1.25152	-2.408063	-1.621297

Table S9: Cartesian coordinates (x,y,z) for the optimized geometry of $^{16}\text{Fnac}_2\text{CuCO}$.

Cu	-0.000033	-0.853792	-0.000007
F	-2.103512	3.927592	0.161582
F	-3.228015	2.370145	1.166406
F	-3.238987	2.500941	-1.010203
F	2.10358	3.927597	-0.159376
F	3.23921	2.500019	1.011123
F	3.227824	2.370857	-1.165603
F	-2.676619	-0.505967	2.357411
F	-5.086314	-1.757739	2.357071
F	-6.433202	-2.128057	0.010223
F	-5.35814	-1.22923	-2.333924
F	-2.949061	0.021771	-2.332615
F	2.948486	0.019382	2.33286
F	5.357597	-1.231683	2.333486
F	6.43324	-2.128015	-0.0113
F	5.086987	-1.755168	-2.358137
F	2.677291	-0.503404	-2.357774
O	-0.000328	-3.771612	-0.001356
N	-1.460114	0.372608	0.01472
N	1.460102	0.372546	-0.014326
C	-1.256403	1.686601	0.028846
C	0.000017	2.305214	0.00044
H	0.00005	3.381792	0.000652
C	1.256409	1.68655	-0.028114
C	-2.465194	2.635747	0.086101
C	2.465227	2.635685	-0.084935
C	-2.76829	-0.181872	0.016605
C	-3.335617	-0.662412	1.200979
C	-4.564797	-1.313984	1.208944
C	-5.252433	-1.504468	0.011765
C	-4.704162	-1.043272	-1.182971
C	-3.472639	-0.394027	-1.17252
C	2.768308	-0.181911	-0.016596
C	3.472357	-0.395293	1.172495

C	4.70387	-1.044527	1.182585
C	5.252464	-1.50444	-0.012514
C	4.565164	-1.312666	-1.209666
C	3.33596	-0.661111	-1.201333
C	-0.000184	-2.625876	-0.000685

Table S10: Cartesian coordinates (x,y,z) for the optimized geometry of $^{17}\text{Fnac}_2\text{CuCO}$.

Cu	0.000034	-0.918495	-0.000746
O	-0.001173	-3.838314	-0.000654
C	-2.370233	2.644366	0.575668
N	-1.457628	0.315437	0.157691
F	0.000047	3.580916	-0.000296
F	3.501963	2.041097	-0.988396
C	0.000066	2.219798	-0.000275
F	2.678445	3.421473	0.472741
C	-1.258436	1.631396	0.216755
N	1.457684	0.315378	-0.158281
F	-6.314247	-2.376777	-0.16746
C	1.258571	1.631389	-0.217094
F	-1.970104	3.427774	1.591417
C	-2.736032	-0.281247	0.11554
F	-2.678614	3.421544	-0.472371
C	2.370513	2.644375	-0.575519
F	1.970778	3.42788	-1.591346
C	-4.863389	-0.704119	-1.000258
F	-4.536074	-2.961558	1.823923
C	-5.162618	-1.707305	-0.079679
F	-2.195031	-1.615959	1.999218
C	-4.256335	-2.00242	0.936367
F	-3.38636	0.94655	-1.797678
C	-3.057761	-1.301676	1.017515
F	-5.726086	-0.418658	-1.979745
C	2.736085	-0.281303	-0.115657
F	3.385576	0.946187	1.798049
C	3.058194	-1.301618	-1.017637
F	5.72523	-0.419027	1.980917
C	4.256738	-2.002353	-0.936075
F	6.314164	-2.376875	0.168574
C	5.162583	-1.707376	0.080407
F	4.536884	-2.961393	-1.823599
C	4.862968	-0.704329	1.001001
F	2.195912	-1.615746	-1.999775
C	-0.000592	-2.693569	-0.000907
C	3.661211	-0.012858	0.902008
F	-3.501548	2.041041	0.988957
C	-3.6616	-0.012661	-0.90169

VIII. References

- [1] K. Huse, C. Wölper and S. Schulz, *Eur. J. Inorg. Chem.*, 2018, 3472.
- [2] A. E. Reed, L. A. Curtiss and F. Weinhold, *Chem. Rev.*, 1988, **88**, 899.
- [3] A. D. Becke, *J. Chem. Phys.*, 1993, **98**, 5648.
- [4] C. Lee, W. Yang and R. G. Parr, *Phys. Rev. B*, 1988, **37**, 785.
- [5] S. H. Vosko, L. Wilk and M. Nusair, *Can. J. Phys.*, 1980, **58**, 1200.
- [6] P. J. Stephens, F. J. Devlin, C. F. Chabalowski and M. J. Frisch, *J. Phys. Chem.*, 1994, **98**, 11623.
- [7] M. J. Frisch, G. W. Trucks, H. B. Schlegel, G. E. Scuseria, M. A. Robb, J. R. Cheeseman, G. Scalmani, V. Barone, A. Petersson, H. Nakatsuji, X. Li, M. Caricato, A. V. Marenich, J. Bloino, B. G. Janesko, R. Gomperts, B. Mennucci, H. P. Hratchian, J. V. Ortiz, A. F. Izmaylov, J. L. Sonnenberg, D. Williams-Young, F. Ding, F. Lipparini, F. Egidi, J. Goings, B. Peng, A. Petrone, T. Henderson, D. Ranasinghe, V. G. Zakrzewski, J. Gao, N. Rega, G. Zheng, W. Liang, M. Hada, M. Ehara, K. Toyota, R. Fukuda, J. Hasegawa, M. Ishida, T. Nakajima, Y. Honda, O. Kitao, H. Nakai, T. Vreven, K. Throssell, J. A. Montgomery, Jr., J. E. Peralta, F. Ogliaro, M. J. Bearpark, J. J. Heyd, E. N. Brothers, K. N. Kudin, V. N. Staroverov, T. A. Keith, R. Kobayashi, J. Normand, K. Raghavachari, A. P. Rendell, J. C. Burant, S. S. Iyengar, J. Tomasi, M. Cossi, J. M. Millam, M. Klene, C. Adamo, R. Cammi, J. W. Ochterski, R. L. Martin, K. Morokuma, O. Farkas, J. B. Foresman, and D. J. Fox, Gaussian, Inc., Wallingford CT, 2016].using NBO 6. [E. D. Glendening, J. K. Badenhoop, A. E. Reed, J. E. Carpenter, J. A. Bohmann, C. M. Morales, C. R. Landis and F. Weinhold, Theoretical Chemistry Institute, University of Wisconsin, Madison (2013).
- [8] J. P. Foster and F. Weinhold, *J. Am. Chem. Soc.*, 1980, **102**, 7211.